

**POLYMER BASED EXTRACELLULAR MATRIX
MIMETICS FOR 3D CELL CULTURE**

**A Thesis Submitted to
the Graduate School of Engineering and Science of
Izmir Institute of Technology
in Partial Fulfillment of the Requirements for the Degree of
MASTER OF SCIENCE
in Biotechnology**

**by
Esra TÜRKER**

**July 2018
İZMİR**

We approve the thesis of **Esra TÜRKER**

Examining Committee Members

Assist. Prof. Dr. Ahu ARSLAN YILDIZ
Department of Bioengineering, İzmir Institute of Technology

Prof. Dr. Funda TIHMINLIOĞLU
Department of Chemical Engineering, İzmir Institute of Technology

Assoc. Prof. Dr. Özlem Yeşil ÇELİKTAŞ
Department of Bioengineering, Ege University

04 July 2018

Assist. Prof. Dr. Ahu ARSLAN YILDIZ
Supervisor,
Department of Bioengineering,
İzmir Institute of Technology

Assist. Prof. Dr. Ümit Hakan YILDIZ
Co- Supervisor,
Department of Chemistry
İzmir Institute of Technology

Assoc. Prof. Engin ÖZÇİVİCİ
Head of the Department of Biotechnology
and Bioengineering

Prof. Dr. Aysun SOFUOĞLU
Dean of the Graduate School of
Engineering and Sciences

ACKNOWLEDGEMENTS

Firstly, I would like to mention my deep and sincere gratitude to my supervisor Assist. Prof. Dr. Ahu ARSLAN YILDIZ and co-supervisor Assist. Prof. Dr. Ümit Hakan YILDIZ for their suggestions, guide, encourage and support throughout my Master of Science thesis study. I acknowledge Scientific Research Projects (SRP) for financial support. Center for Material Research (IZTECH-MAM), Biotechnology and Bioengineering Research and Application Center (IZTECH BIOMER) of their high-tech laboratory during my experimental studies.

I am very thankful to my co-workers, Duygu Erdoğan, Cemre Yaşar and Mustafa Umut Mutlu for their encourage and help during my throughout thesis study. Çağatay Saritepe, Nida Demirçak, Müge Yücel, Rumeysa Bilginer, Sezer Özenler and the rest of Biomimetics and BioSens & BioApps groups for their friendship, support, help, patience. I also want to express special thanks to my family for their encouragement, patience and support during my whole education life.

Especially, I would like to offer my special thanks to my family and my second family who is Pınar Şirin and her family. I am very lucky to have their love and patience they show me in my private life as well as my educational life. I dedicate my thesis especially to my mother and father.

ABSTRACT

POLYMER BASED EXTRACELLULAR MATRIX MIMETICS FOR 3D CELL CULTURE

Tissue engineering combines engineering principles and knowledge of life sciences to improve biological substitutes. Three dimensional (3D) supporting structures, namely scaffolds obtained from biomaterials to mimic extracellular matrix (ECM) that provides suitable microenvironment for cell proliferation, migration and differentiation. In this study, poly (L-lactide-co- ϵ -caprolactone) (PLLCL) and collagen type I was used to fabricate scaffold by electrospinning method. In literature, collagen was often dissolved in toxic and harmful solvents that creates the major problem for cell culture applications. To overcome this problem “co-spinning” methodology is utilized for the formation of non-toxic collagen-based ECM mimetic scaffold. Collagen mixed with water-soluble carrier materials which is either polyvinylpyrrolidone (PVP) or polyvinyl alcohol (PVA) and co-electrospinning is carried out with PLLCL. Fabricated scaffolds were immersed into water to remove co-spinning agent; PVA or PVP, so only PLLCL/Collagen remained. PLLCL has homogeneous fibers in a diameter of $1.312 \pm 0.22\mu\text{m}$. The contact angle of PLLCL ($136.6^\circ \pm 2.6$) proved hydrophobic behavior of PLLCL material. The contact angle of the scaffold decreased up to $86.7^\circ \pm 0.1$ confirming that hydrophobic behavior is decreased with the addition of collagen. Also, collagen-containing scaffolds were saturated at lower amount of protein than PLLCL, PLLCL/PVA and PLLCL/PVP scaffolds. Cytotoxicity analysis of scaffolds showed that PVA containing scaffolds had lower viability than PVP containing scaffolds; so most of the cell studies were carried out with PLLCL/ Collagen scaffolds fabricated by PVP co-spinning. Cell proliferation on PLLCL/Collagen scaffolds found to be more favorable than PLLCL and PLLCL/PVP scaffolds.

ÖZET

ÜÇ BOYUTLU HÜCRE KÜLTÜRÜ İÇİN POLİMER ESASLI EKSTRASELLÜLER MATRİKS MİMETİĞİ

Doku mühendisliği, biyolojik oluşumları geliştirmek için mühendislik prensiplerini ve yaşam bilimleri bilgisini birleştirir. İskele olarak adlandırılan üç boyutlu (3D) destekleyici yapılar biyomalzemelerden elde edilerek, hücre çoğalması, göçü ve farklılaşması için uygun mikro ortamı sağlayan hücre dışı matrisi (ECM) taklit ederler. Bu çalışmada, poli (L-laktit-ko-ε-kaprolakton) (PLLCL) ve kolajen tip I, elektro-eğirme yöntemi ile iskeleleri üretmek için kullanılmıştır. Literatürde, kolajen sıklıkla hücre kültürü uygulamaları için önemli bir problem oluşturan zehirli ve zararlı çözücüler içinde çözülmüştür. Bu problemin üstesinden gelmek için toksik olmayan kolajen bazlı ECM mimetik iskele oluşumu için “eş zamanlı eğirme” metodolojisi kullanıldı. Kolajen, suda çözünen taşıyıcı polivinilpirrolidon (PVP) veya polivinil alkol (PVA) ile karıştırılarak PLLCL ile eş zamanlı elektro-eğirme işlemi uygulandı. Üretilen iskeleden PVA veya PVP eş zamanlı eğirme ajanı uzaklaştırılarak sadece PLLCL/ Kolajen kalır. PLLCL, $1.312 \pm 0.22\mu\text{m}$ çapında homojen liflere sahiptir. PLLCL’un temas açısı ($136.6^\circ \pm 2.6$), mazlemenin hidrofobik özelliğini kanıtlamaktadır. İskelenin temas açısı $86.7^\circ \pm 0.1$ ’ye düşmesi, kolajenin ilavesiyle hidrofobik davranışın azaldığını doğrulamaktadır. Ayrıca protein adsorbsiyon analizinde kolajen içeren iskeleler, PLLCL, PLLCL/PVA ve PLLCL/PVP iskelelerine göre daha düşük miktarda protein ile doyurulmuştur. İskelelerin sitotoksitesite analizi, PVA içeren iskelelerin, PVP içeren iskelelerden daha düşük canlılığa sahip olduğunu göstermiştir; bu nedenle hücre çalışmalarının çoğu PVP varlığında eş zamanlı eğirme ile üretilen PLLCL / Kolajen iskeleleri ile gerçekleştirilmiştir. PLLCL / Kolajen iskelelerinde hücre çoğalması PLLCL ve PLLCL / PVP iskelelerine göre daha uygun bulunmuştur.

TABLE OF CONTENTS

LIST OF FIGURES	viii
LIST OF TABLES	xi
CHAPTER 1. INTRODUCTION	1
1.1. Scope of Thesis	1
1.2. Tissue Engineering	1
1.2.1. Extracellular Matrix	3
1.3. Biomaterials for Tissue Engineering	7
1.3.1. Natural Polymers	7
1.3.2. Synthetic Polymers	9
1.3.3. Composite Polymers	12
1.4. Scaffold Fabrication Techniques	13
1.4.1. Solvent Casting/ Particle Leaching Method	14
1.4.2. Gas Foaming Method	14
1.4.3. Freeze-Drying Method	15
1.4.4. Rapid Prototyping Technique (RP)	16
1.4.5. Electrospinning	16
CHAPTER 2. MATERIALS AND METHODS	20
2.1. Materials	20
2.2. Methods	21
2.2.1. Fabrication of PLLCL Scaffold	21
2.2.2. Fabrication of PLLCL/ PVA/ Collagen and PLLCL/ PVP/ Collagen Scaffolds	21
2.2.3. Characterization Tests	23
2.2.3.1. Scanning Electron Microscope (SEM) Analysis	23
2.2.3.2. Collagen Immunostaining Analysis	23
2.2.3.3. Fourier Transform Infrared - Attenuated Total Reflectance Spectroscopy (FTIR-ATR) Analysis	24
2.2.3.4. Contact Angle Analysis	24

2.2.3.5. Protein Adsorption Assay	25
2.2.3.6. Mechanical Analysis	26
2.2.3.7. Hydrolytic and Enzymatic Biodegradation Study	27
2.2.3.8. <i>In vitro</i> Cell Culture Studies	27
2.2.3.8.1. Cell Seeding on PLLCL/Collagen Scaffolds	28
2.2.3.8.2. Cell Proliferation and Viability on PLLCL/ Collagen Scaffolds	28
2.2.3.8.3. Morphological Analysis of Cell Proliferations on PLLCL/Collagen Scaffolds.....	29
 CHAPTER 3. RESULT AND DISCUSSION	 30
3.1. Characterization of PLLCL Nanofibers.....	30
3.2. Characterization of PLLCL/ Collagen Scaffolds.....	32
3.3. Immunostaining of PLLCL/Collagen Scaffolds.....	35
3.4. FTIR-ATR Analysis of PLLCL/Collagen Scaffolds	36
3.5. Contact Angle of PLLCL/Collagen Scaffolds	39
3.6. Protein Adsorption of PLLCL/Collagen Scaffolds.....	41
3.7. Mechanical Characterization with Tensile Test	43
3.8. Hydrolytic and Enzymatic Biodegradation of PLLCL Scaffolds.....	45
3.9. <i>In vitro</i> 3D Cell Culture Studies	49
3.9.1. <i>In vitro</i> Proliferation Assay on PLLCL/Collagen Scaffolds.....	49
3.9.2. Cell Viability Assay on PLLCL/Collagen Scaffolds.....	51
3.9.3. SEM Cell Analysis of Cell Attachment on PLLCL/Collagen Scaffolds	55
 CHAPTER 4. CONCLUSION	 58
 REFERENCES	 60

LIST OF FIGURES

<u>Figure</u>	<u>Page</u>
Figure 1.1. Key elements of tissue engineering.....	2
Figure 1.2. Schematic of extracellular matrix structure and its components.....	3
Figure 1.3. Schematic of collagen molecular structure. Gly-X-Y containing α -chain (1) forms a triple helical structure (2). Triple helical structures assemble and form collagen fibrils (3). The combination of collagen fibrils assembles to form collagen fibers (4)	4
Figure 1.4. Poly (α -hydroxy esters) structures where non-biodegradable polymers are a) PEO, b) PVA, c) poly-HEMA, d) PANIPAM; and biodegradable polymers are e) PGA, f) PLA, g) PLGA, h) PLLCL, i) polyanhydride, j) PCL.....	9
Figure 1.5. PLLCL synthesis from L-lactide and ϵ -caprolactone via $\text{Sn}(\text{Oct})_3$ catalyst.....	11
Figure 1.6. Schematic representation of solvent casting/particle leaching method.....	14
Figure 1.7. Scaffold fabrication by gas foaming technique.....	15
Figure 1.8. Schematic of freeze-drying method	15
Figure 1.9. Schematic illustration of electrospinning system that composed of a pump system, syringe, conducting surface and power supply.....	17
Figure 1.10. Schematic of co-electrospinning set up.....	18
Figure 2.1. Electrospinning device (Inovenso NE300).....	21
Figure 2.2. Co-electrospinning set up with two nozzles and two pump systems.	22
Figure 3.1. Solutions of PLLCL in varied DCM: DMF ratio, a) 2.5:2.5 mL, b) 3.5:1.5 mL and c) 4.5:0.5 mL, d) SEM micrograph of porous PLLCL fiber in 4.5:0.5mL DCM: DMF	30
Figure 3.2. SEM images of electrospun PLLCL scaffolds and fiber distribution in varied concentration of PLLCL a) 5%wt, b) 8%wt and c) 10%wt.....	31
Figure 3.3. SEM micrographs of co-electrospun scaffolds right after spinning (without washing with deionized water), a) PLLCL/ PVA/ 0.4%Collagen, b) PLLCL/PVP/0.8%Collagen and c) PLLCL/ PVP/ 1%Collagen.....	33

Figure 3.4. SEM micrographs of co-electrospun scaffolds prior to removal of sacrificing agents (after washing with deionized water), a) PLLCL/0.4%Collagen, b) PLLCL/0.8%Collagen and c) PLLCL/1%Collagen	34
Figure 3.5. Fluorescence microscopy images of immunostained scaffolds, a) PLLCL, b) PLLCL/ PVP, c) PLLCL/PVP/0.8%Collagen, d) PLLCL/0.8%Collagen (after removing PVP), e) PLLCL/PVP/1%Collagen, and f) PLLCL/1%Collagen (after removing PVP)	35
Figure 3.6. FTIR spectra of pristine Collagen, PLLCL, PVP and PVA.	37
Figure 3.7. FTIR spectra of PLLCL/ PVA/ 0.4%Collagen (black) and PLLCL/0.4%Collagen (after PVA removal) (red) scaffolds.	38
Figure 3.8. FTIR spectra of PLLCL/PVP/0.8%Collagen and PLLCL/PVP/1%Collagen (black), PLLCL/0.8%Collagen (after PVP removal) and PLLCL/1%Collagen (after PVP removal) (red) scaffolds.....	38
Figure 3.9. Standard calibration curve of BSA.....	41
Figure 3.10. Solubilizing adsorbed BSA on PLLCL scaffold with Tween 80, Tween 20, TritonX-100 and SDS.	42
Figure 3.11. Weakly adsorbed BSA on scaffolds.....	43
Figure 3.12. Solubilized BSA on scaffolds.....	43
Figure 3.13. Stress-strain curve of PLLCL, PLLCL/ PVP, PLLCL/ PVP/ 0.8%Collagen, PLLCL/ %0.8Collagen (after PVP removal), PLLCL/ PVP/ 1%Collagen and PLLCL/1%Collagen (after PVP removal).	45
Figure 3.14. <i>In vitro</i> biodegradation analysis of PLLCL in 20week incubation period, a) weight loss and b) porosity against weeks.....	46
Figure 3.15. SEM micrographs of hydrolytic degradation of PLLCL a) 9 th week, b) 13 th week, c) 17 th week and d) 20 th week	47
Figure 3.16. SEM micrograph of enzymatic degradation of PLLCL a) 9 th week, b) 13 th week, c) 17 th week and d) 20 th week.....	48
Figure 3.17. MTT assay results of NIH3T3 cell proliferation on PLLCL, PLLCL/ PVA, PLLCL/PVA/0.4%Collagen, PLLCL/0.4%Collagen (after removing PVA), PLLCL/PVP, PLLCL/PVP/0.4%Collagen, PLLCL/0.4%Collagen (after removing PVP) scaffolds in 1, 3, 5 and 7 days cell culture periods.	49
Figure 3.18. Alamar blue assay results of NIH3T3 cell proliferation on PLLCL, PLLCL/PVP, PLLCL/PVP/0.8%Collagen, PLLCL/0.8% Collagen	

(after removing PVP), PLLCL/PVP/1%Collagen and PLLCL/1%Collagen (after removing PVP) scaffolds for 1, 3, 5 and 7day cell culture period.	51
Figure 3.19. Fluorescence microscope images of live/ dead assay on PLLCL, PLLCL/PVA, PLLCL/PVA/0.4%Collagen, PLLCL/0.4%Collagen (after removing PVA) and PLLCL/PVP, PLLCL/PVP/0.4%Collagen, PLLCL/0.4%Collagen (after removing PVP) scaffolds for 1, 3, 5 and 7day cell culture periods (scale bar 100µm). Green represents live cells, red represents dead cells.	53
Figure 3.20. Fluorescence microscope images of live/ dead assay on PLLCL, PLLCL/PVP, PLLCL/PVP/0.8%Collagen, PLLCL/0.8%Collagen (after removing PVP) and PLLCL/PVP/ 1%Collagen, PLLCL/1%Collagen (after removing PVP) scaffolds for 1, 3, 5 and 7day cell culture periods (scale bar 100µm). Green represent live cells, red represents dead cells.	54
Figure 3.21. Fluorescence microscope images of live/ dead assay on PLLCL, PLLCL/PVP, PLLCL/PVP/1%Collagen and PLLCL/1%Collagen (after removing PVP) scaffolds for 1, 7, 11 and 15day cell culture periods (scale bar: 100µm). Green represent live cells, red represents dead cells.	55
Figure 3.22. Cell attachment and proliferation behavior of NIH 3T3 cells on PLLCL/0.4%Collagen (after PVP removal) scaffolds in a) 1 st day, b) 3 rd day, c) 5 th day and d) 7 th day cell culture periods.	56
Figure 3.23. SEM micrograph of NIH 3T3 cell attached on PLLCL/0.4%Collagen fibers.	57

LIST OF TABLES

<u>Table</u>	<u>Page</u>
Table 2.1. Bovine serum albumin (BSA) standards preparation	25
Table 3.1. Contact angle of PLLCL and PLLCL/Collagen scaffolds with and without PVA. Results reported as mean \pm SD for three measurements.....	40
Table 3.2. Contact angle of PLLCL and PLLCL/Collagen scaffolds with and without PVP. Contact angles reported as mean \pm SD for three measurements.....	40
Table 3.3. Tensile tests result of scaffolds. Results reported as mean \pm SD for four measurements.....	44

CHAPTER 1

INTRODUCTION

1.1. Scope of Thesis

Poly(L-lactide-co- ϵ -caprolactone) (PLLCL) and collagen type I biocomposite three-dimensional (3D) scaffold was used to mimic physical and biochemical properties of natural extracellular matrix (ECM). PLLCL/Collagen scaffold was fabricated by electrospinning method. In literature, the solubility and process of collagen is a big issue where toxic solvents were used, so collagen was dissolved in 0.1M acetic acid and mixed with water-soluble polyvinylpyrrolidone (PVP) and polyvinyl alcohol (PVA). Here either PVP or PVA was utilized as a carrier material and co-electrospinning was achieved with PLLCL. Later, carrier material was removed from scaffolds via solubilizing with water, and remaining PLLCL/Collagen scaffold was used for further 3D cell culture studies.

1.2. Tissue Engineering

Every year, millions of health problems arises due to lost or damaged tissues, which causes significant clinical issues.¹⁻² Organ transplantation is performed for tissue and organ loss by using mechanical devices and surgical intervention. For a certain time, these methods saved many lives, however, they still contain deficiencies and causes unwanted results. In each year, demand is increasing for an organ donation. Most patients die while waiting because the number of patients donating the organs cannot keep up with the demand. Apart from that, surgical interventions can cause long-term problems such as surgical treatment of incontinence is one of the reason of colon cancer.³ Also, mechanical devices are not able to perform whole function of an organ, so they cannot prevent patients to become progressively worse. To overcome these problems; tissue engineering approaches provides better and functional alternatives. Tissue engineering is a multidisciplinary field that combines many disciplines and sub-disciplines like engineering, material science, life science etc. to improve biological

substituent. The major aim of the tissue engineering is to regenerate damaged tissues and organs, and to maintain or improve their functions.⁴⁻⁵

Three main pillars of tissue engineering can be classified in 3 categories (Figure 1.1):⁶ *i*) Cells; the most important component of artificial tissues and organs that provide the necessary function, *ii*) Supporting molecules; relying on purification and wide range production of biomolecules such as signaling molecules, growth factors etc. for the formation and development of functional tissue constructs, *iii*) Scaffold materials; 3D structural materials that provides suitable environment for cell proliferation, nutrient transport and waste removal. Scaffold materials generally constructed from natural or synthetic polymer materials.³ Recently, mimicking the ECM content and structure become a popular approach since it provides natural microenvironment for cells and tissues.⁷⁻¹¹

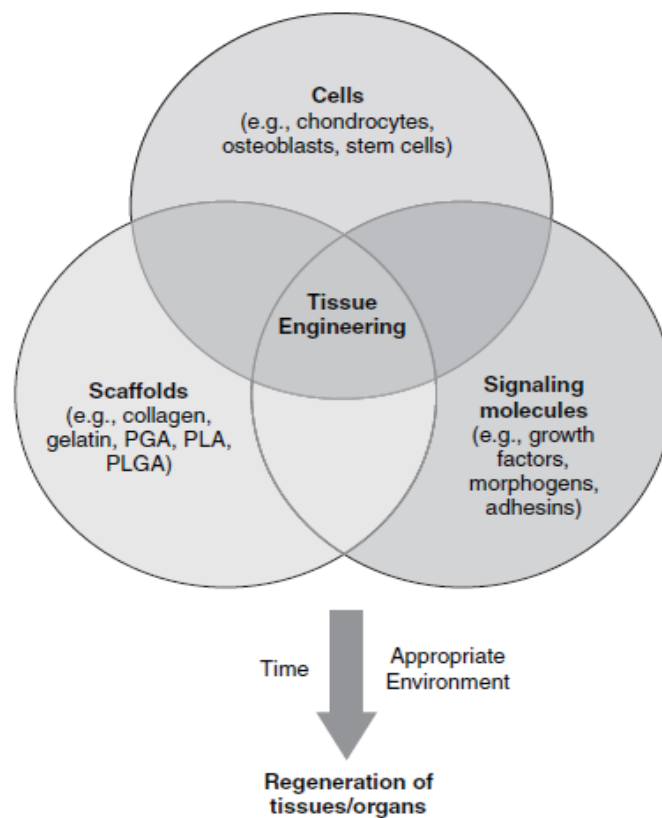


Figure 1.1. Key elements of tissue engineering.⁶

1.2.1. Extracellular Matrix

Cells are surrounded by 3D complex mixture of fibrillar structures of collagen, elastin, proteoglycans and non-collagenous glycoproteins, glycosaminoglycans which is amorphous matrix called ECM (Figure 1.2).¹²⁻¹³ It exists within all native tissues and organs which is a non-cellular component and it starts biochemical and biomechanical signaling which is necessary for tissue morphogenesis, differentiation and hemostasis.¹⁴ ECM content varies from tissue to tissue, even it may vary within the same tissue owing to structure and function of tissues and macromolecules; such as bone that is composed of mineralized ECM. Not only all ECM content but also a single ECM molecule may vary according to structural and functional requirements. For example, cells of ligaments and tendons secrete collagen proteins that provide resistance. On the other hand, fibrillar form of collagen at intestine give the specific spiral shape that is secreted for constructional purposes.¹⁵

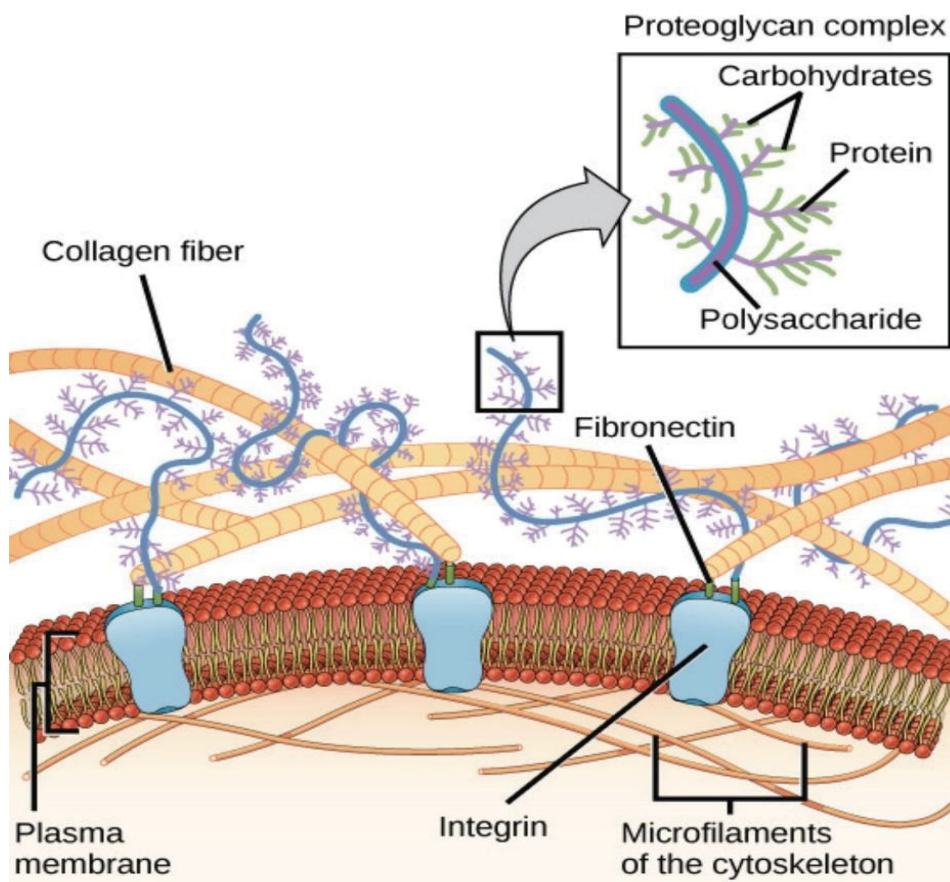


Figure 1.2. Schematic of extracellular matrix structure and its components.¹³

Fibrous proteins such as collagen provides constructional support and strength to the cells. Collagen is one of the widespread existence protein of ECM.¹⁶⁻¹⁷ It is the main protein of vertebrates and generally secreted from fibroblasts. Arrangement and alignment of collagen fibrils into layers provided by fibroblasts while force is applied on the matrix. Currently, more than 28 types of collagen exist that have different functions.¹⁸⁻²⁰ According to their size, structure, function and distribution in tissue, collagens differ, however the main backbone of collagen molecules are composed of Glycine-X-Y repeating units forming triple helix structure (Figure 1.3). In particular, proline and hydroxyproline are occupying the X and Y positions. Due to high amount of glycine, proline and hydroxyproline content, α -chains form left-handed single helices. Every third residue of α -chain has glycine that has hydrogen atom side chain, so intramolecular hydrogen bonding leads to formation of triple helix structure. Large side groups of proline and hydroxyproline turn to outside and help with tight packing of α -chains.

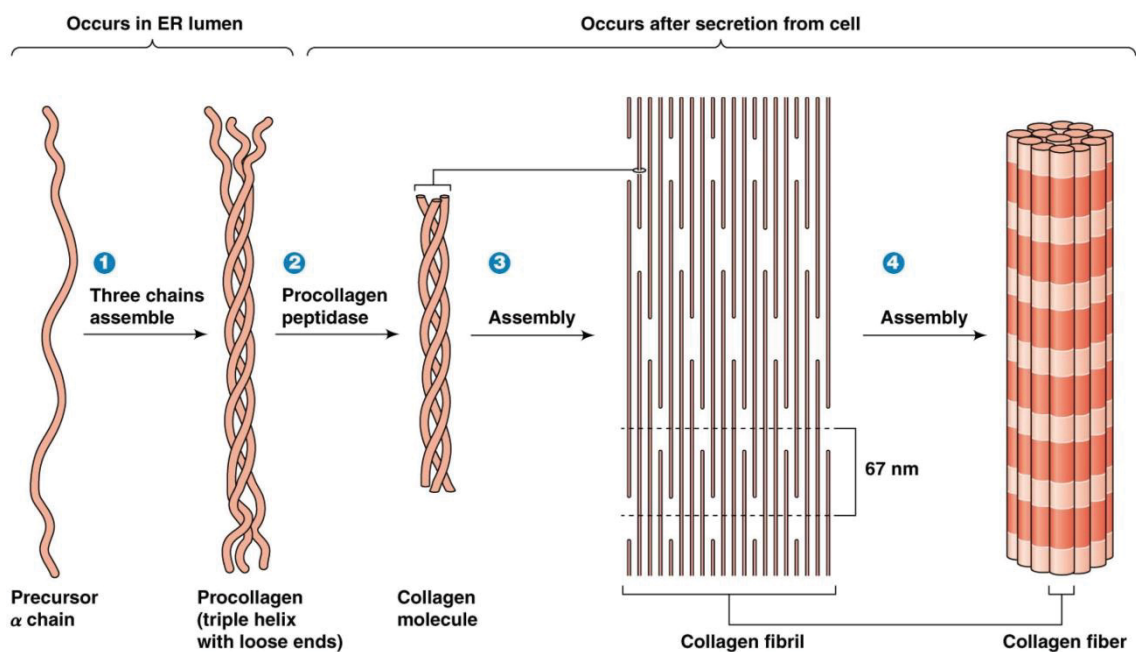


Figure 1.3. Schematic of collagen molecular structure. Gly-X-Y containing α -chain (1) forms a triple helical structure (2). Triple helical structures assemble and form collagen fibrils (3). The combination of collagen fibrils assembles to form collagen fibers (4).²¹

Procollagen metalloproteinases split procollagen peptides which is processed in extracellular matrix to obtain collagens “fibrillar structures” (Type I, II, III, V, XI, XXIV, XXVII).^{17,22} Another form of collagen is “sheet-forming collagen” that collagen

fibrils are assembled as network-like structures (Type VIII and X). Basal membrane is one of the examples of a sheet-forming collagen made of type IV collagen, which is highly flexible. “Anchoring” or “linking collagen” is another type of collagen that connects with fibrillar surfaces, especially type VI, IX, XII and XIV collagens are classified under this group. Collagen type I is the most commonly used and abundant one in the body and it mostly provides tensile strength and stability.²³ Triple helix of collagen type I consist of two identical $\alpha 1(I)$ -chain and $\alpha 2(I)$ -chain. It mainly exists at tendons, ligaments, skin, cornea and other connective tissues except cartilage and brain.

Another fibrillar protein of ECM is elastin that associates with collagen and provide stretching ability for tissues like skin, blood vessels and lungs. Tissues are recoiled based on elastic properties of elastin fibers. Collagen fibrils restricts elastin stretching because of tight association with each other.²⁴⁻²⁵ The soluble precursor “tropoelastin” is a protein composed of hydrophobic lysine domains which ensures crosslink formation from one lysine domain to another by lysyl oxidase(LOX) enzyme and formed elastin fibers.

Fibronectin (non-collagenous) is also an important component of ECM that controls the cellular behavior such as differentiation, migration and growth as well the presence of specific binding sites provides adhesion of cells.^{15-16, 26} Laminin and fibronectin are the main ECM proteins that mediates the cell adhesion. Fibronectin is in fibrillar form which has different binding domains responsible from binding to cell surface receptors. Two types of fibronectin exist: soluble one available in blood plasma and insoluble one that is available in ECM. Integrins bind to fibronectin via Arg-Gly-Asp (RGD) peptides, which triggers the cell adhesion and this sequence is also important for cell growth. Laminin; an important member of the ECM that supports cell adhesion, is found in every basal tissue. It has three short and one long arm that form a big quaternary structure. With the support of its arms, it connects with other molecules and plays an important role in cell differentiation, proliferation and migration.

Proteoglycans (PGs) fill the gaps of ECM in a hydrated gel form and ensure binding, buffering and resistance against force.^{16, 27-28} It is made up of a core protein where glycosaminoglycan chains (GAGs) covalently linked on it. Classification of PGs rely on core protein localizations and configuration of GAGs. The GAG chains in the core protein is composed of polysaccharides that occur in recurrent disaccharides. These variabilities of disaccharides provide heterogeneous design where each chain has distinct functions. Big fraction of the ECM composed of PGs, they are present not only

in ECM but also on the cell surface and some parts of the cells. It participates into certain cellular functions such as cell signaling, proliferation, differentiation, attachment by binding to growth factors, ECM molecules and cell surface receptors via their core proteins or GAGs side chains. Moreover, PGs contribute to the formation of complex ECM structure by binding to the ECM and cells are embedded within. Additionally, non-fibrillar parts that are formed by mostly glycosaminoglycan adjusts turgor pressure, homogeneous intercellular connections, regulate binding and growth factor activity.²⁹

Collagen type I, which is commonly found in fibrillar structure, and collagen type II, found in cartilage, are major proteins that are widely present in ECM.¹⁶ These constructs produce larger fibril structures, which are intertwined with other collagens, ECM proteins and PGs structures. These large fibrillar and molecular organization associate with ECM molecules and form the large 3D network of ECM. Integrins³⁰⁻³¹ (syndecan, discoidin domain receptors)³²⁻³³ mediate signaling by interacting with ECM network. These signals guide cells to change their attitudes and functions. Epithelial, endothelial, fibroblasts and immune cells secrete macromolecular networks through multiple signals and forms ECM structures. Any change of ECM molecules influences whole structure and biochemical features of the network.

Until the importance of ECM was noticed, it was not possible to maintain differentiation and function of growing cells without deteriorating their properties.³⁴ The fact that cells cannot maintain their normal behavior in a 2D culture environment due to the absence of ECM, which provides a 3D environment.³⁵ Therefore, researchers have been trying to make a similar complicated structure of the ECM *in vitro*.

To reach that ultimate aim 3D cell culture system and methods has been developed that mimic the ECM structure and function.³⁶⁻³⁸ Traditional two-dimensional (2D) cell culture methods on tissue culture plates do not reflect the exact morphology of *in vivo* microenvironment, so instead of 2D techniques, 3D cell culture techniques were started to use to mimic natural ECM microenvironment. In 3D matrix, cells are grown more easily forming tissue-like structures as similar as native tissues. Currently, many methodologies are used to perform 3D cell cultures, some of which can be classified as organotypic explant cultures, cell spheroids, bioreactor methods, polarized epithelial cell culture methods, and biomarker-based cell culture methodologies.³⁹⁻⁴¹

1.3. Biomaterials for Tissue Engineering

Through tissue engineering process cells are detached from a patient and are grown in 3D scaffold that mimic natural ECM, and then the scaffold is implanted to a host to renew tissue formation in the matrix that degrades over time. To accomplish effective recovery of harmed organs or tissues in light of the tissue engineering, a few components ought to be considered including scaffolds materials which present physical support for cell growth, differentiation and also growth factors that provide cellular functions. Thus, fabrication and formation of a scaffold meet requirements that natural ECM provides to cells.⁴²⁻⁴³ A scaffold should have following properties: *i)* to be made from a suitable material that is biodegradable, so real tissue will take place of the scaffold, *ii)* well designed interconnected pores for tissue integration, *iii)* should be biocompatible to prevent any adverse effects, *iv)* should possess suitable mechanical properties, *v)* appropriate surface chemistry in order to provide cellular differentiation, proliferation and attachment, *vi)* should be fabricated in different shape and sizes.

1.3.1. Natural Polymers

Natural polymers are advantageous biomaterials for tissue engineering applications because they provide biological environment and can be metabolized over time.^{4, 44} Most of them are derived from natural ECM proteins (collagen, hyaluronic acid, fibrinogen, elastin, keratin, actin, silk), polysaccharides (chitin, cellulose, glycosaminoglycans) or polynucleotides (DNA, RNA). Toxicity problem, chronic inflammatory reaction and recognition from cells are not as problem as synthetic polymers. Additionally, they can be immunogenic. These materials demonstrate perfect biocompatibility and viability, but their mechanical stability and physical capabilities are restricted. Further, natural originated enzymes can degrade the natural polymers and finally metabolize in a body. Depending on applications, this ability can be advantageous or disadvantageous. Because for a long-term regeneration processes, the strength of the scaffold going to decrease and metabolically removed from the host before tissue regeneration is completed. But it is suitable for short-term temporary applications.

Collagen is the most abundant protein found in living organisms, which is also commonly used in tissue engineering applications. It has an active role in tissue and organ formation, even at different cellular functions. It has good biodegradability, biocompatible properties in contrast to other natural polymers which are albumin and gelatin. Due to its fibrillar structure provide physical strength to a scaffold.⁴⁵ Collagen is one of the most widely used and distributed protein in the body, so it is extracted from many animals.⁴⁶ In tissue engineering applications bovine skin and tendons, rat tail and porcine skin are some of the mostly used collagen sources.

Collagen can interact with cells, directly and indirectly. Interior of the collagen has Asp-Gly-Glu-Ala peptide sequence where cell receptors are recognized and direct cell-collagen interaction.⁴⁶⁻⁴⁷ Whereas fibronectin interacts with integrin by its RGD peptide bond in the structure and indirectly associated with cell-collagen connection. Collagen receptors and binding molecules are important by selecting the collagen for collagen-based biomaterials. Xiang et al. were studied the reaction of rat myocardial scar tissue by producing a hybrid scaffold composed of two natural materials which is collagen type I and glycosaminoglycans (GAG)⁴⁸. Scaffolds were prepared with two crosslink methods and evaluate their applicability by utilizing collagen-GAG scaffold as a transport vehicle for bone marrow derived mesenchymal stem cells (MSCs). MSCs were recognized at the connective tissues where cells migrate to the defect side of the heart wall. Besides, collagen-GAG scaffolds were applied as a regeneration scaffold on dermis,⁴⁹ peripheral nerve⁵⁰ and successful regenerations result were obtained. Another study was investigated by Zhang et al. where cartilage formation was examined *in vitro* without using any growth factor. They were developed a collagen type I hydrogels that induce bone marrow mesenchymal stem cells (BMSCs) to chondrogenic lineage.⁵¹ Thus, cartilage regeneration can be accomplished by this application with native induction of collagen. In previous studies, valvular interstitial cells (VICs) have been worked to adhere on laminin coated surfaces or RGD modified fibronectin surfaces but the results were not as expected. Cell adhesion and proliferation was limited, and morphology was different than expected. Therefore, Masters et al. have studied on photopolymerizable hyaluronic acid hydrogels where VICs spread and proliferate in a short time.⁵² Moreover, Alsberg et al. have developed a fibrin based biomaterial for magnetic self-assembly.⁵³ Thrombin coated magnetic beads were located at air-liquid interface of a fibrinogen solution. For a while, enzymatically cleaved fibrinogen release fibrin and magnetically guided fibrins self-assembly into 3D structure.

1.3.2. Synthetic Polymers

Synthetic polymers are easy to process and handle. Compared to natural polymers that are expensive, influence from cross-contamination and varies from batch-to-batch,^{6, 54-55} synthetic polymers provide better alternatives. Synthetic scaffolds are easy to produce by using various methods, as well as physical and mechanical abilities can be adjusted regarding to a tissue region to be applied. Additionally, they ensure short-term or long term mechanical strength until tissue accomplish regenerations.⁵⁶⁻⁵⁷ They are batch-to-batch invariable, biological inert and can be metabolized after tissue regenerations. They are including hydrolytic or enzymatic cleavage bonds, so polymer erosion occurs and can be metabolically removed from the body. They are biocompatible that has no foreign effects on the implanted sides.

Synthetic polymers are divided into two groups as biodegradable and non-biodegradable (Figure 1.4).

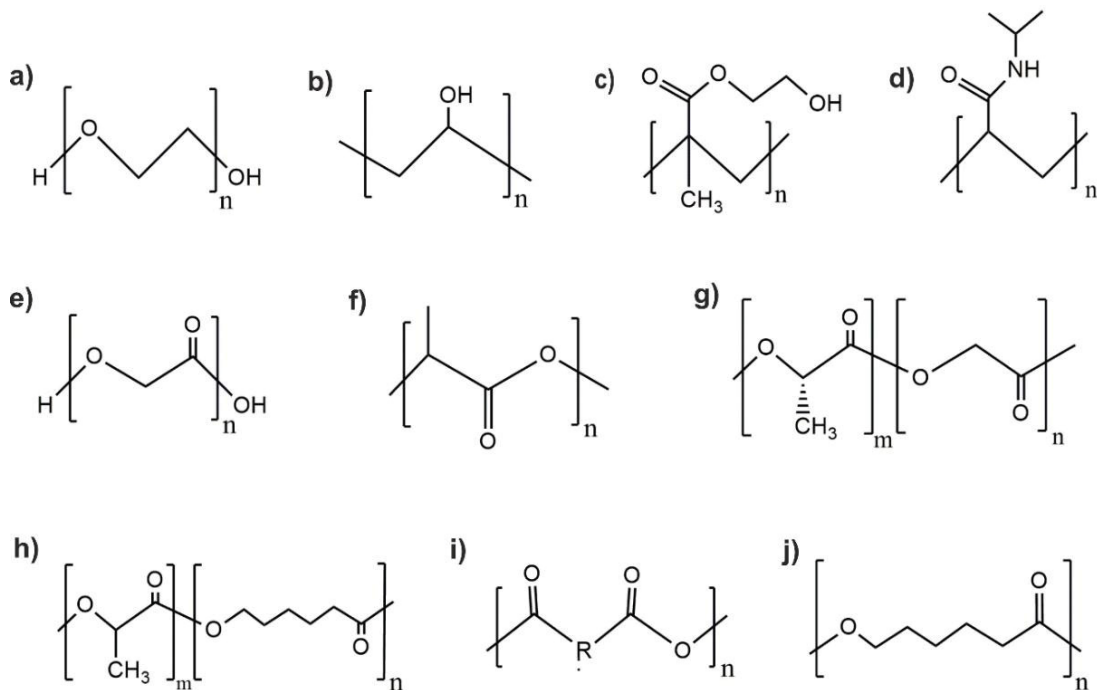


Figure 1.4. Poly (α -hydroxy esters) structures where non-biodegradable polymers are a) PEO, b) PVA, c) poly-HEMA, d) PANIPAM; and biodegradable polymers are e) PGA, f) PLA, g) PLGA, h) PLLCL, i) polyanhydride, j) PCL.

Some of non-biodegradable materials are poly (ethylene oxide) (PEO), polyvinyl alcohol (PVA), poly (hydroxyethyl methacrylate) (poly-HEMA), and poly(N-isopropylacrylamide) (PANIPAM). Due to their biodegradation ability poly (α -hydroxy esters) family has been heavily used such as polyglycolide (PGA), polylactide (PLA), polycaprolactone (PCL) and their co-polymers poly(L-lactide-co-glycolide) (PLGA), poly(L-lactide-co- ϵ -caprolactone) (PLLCL), polyanhydride, etc.

Poly (α -hydroxy esters) are one of the mainly used synthetic polymer family in tissue engineering applications among other polymer groups.^{6, 58-59} They are approved by Food and Drug Administration (FDA) for human clinical use. In tissue engineering these polymers are widely used as a scaffold due to their controllable biodegradation, easy handling, and good biocompatibility features. Ester bond provides easy degradation; so degraded products can be easily metabolized from the body. For example, PGA degradation occurs both hydrolytically and enzymatically. The resulting glycolic acid after degradation enter the tricarboxylic acid (TCA) or urea cycle and is eliminated as carbon dioxide and water. Further, PLA can be naturally metabolized from a human body because it is a product of anaerobic metabolism. It goes through the TCA cycle lead to excreted as carbon dioxide and water. The copolymerization of PGA and PLA that is PLGA has a controllable degradation rate as well as controllable mechanical and physical properties. According to their monomer composition, molecular weight and degradation time can be adjusted.

Properties of poly lactic acid (PLA) changes according to its chirality as D (-), L (+) and D, L where D and L isomers are semi-crystalline, D,L is amorphous polymers.⁶⁰ PLLA is a tough material and has a 65°C glass transition temperature 170-180°C of melting temperature. On the other hand, PDLLA is an amorphous material and softer than PLLA that have 50-60°C of glass transition temperature. Therefore, degradation of PDLLA is faster than PLLA around 2-13 months. Also, PLLA is preferred because it can be easily metabolized from human body. Yang et al. were used PLLA and fabricated 3D porous scaffold by phase separation method.⁶¹ Concentration change affect the diameter and porosity of the scaffold which is important for cells behaviors. Later neural stem cells (NSCs) were seeded, differentiation and outgrowth of NSCs cells were observed in the 3D scaffold. These results emphasize the importance of the 3D PLLA scaffold as carrier for nerve tissue regeneration applications.

Poly(ϵ -caprolactone) (PCL) is another polyester family member that is common used in tissue engineering. It is produced from ring opening polymerization of ϵ -

caprolactone.^{60, 62} Stannous octoate is the catalyzer that provide polymerization of the reaction. It is a semi-crystalline polymer that have -60°C of glass transition temperature and melting point at $59-64^{\circ}\text{C}$. Ester linkage provide hydrolytic degradation of the polymer. After degradation, ϵ -hydroxycaproic acid is obtained and metabolized via TCA or renal secretion. Due to its aliphatic chain and crystallinity, degradation rate is much slower than PLLA which is approximately 2 years. It can be advantageous to have a low rate of degradation according to the use of field.⁶³⁻⁶⁵ In recent studies, Ruckh et al. fabricated a PCL scaffold by electrospinning method with combining oleic acid sodium salt.⁶⁶ Marrow stromal cells (MSCs) were examined in osteogenic media to investigate their osteoblastic attitudes. Smooth PCL and nanofibrous PCL were compared according to MSCs adhesion and proliferation. Fibrous structure provided better cellular activity which was supported by increasing alkaline phosphate activity and calcium phosphate mineralization for 3 weeks of culture. Additionally, PLLA and PCL blended scaffolds were also used for 3D cell cultures which was fabricated by Chen et al. by using electrospinning method.⁶⁷ Via changing weight percentages of PLLA and PCL, optimizations studied have been performed to obtain suitable diameter, pore size, morphology. After characterization, biocompatibility of the 3D scaffold was determined by using human adipose-derived stem cells (*hASCs*). According to percentages of components, cellular activities were compared, and suitable scaffold was optimized for further applications.

Copolymer of PLLA and PCL called as poly(L-lactide-co- ϵ -caprolactone) (PLLCL) is synthesized by stannous octoate ($\text{Sn}(\text{Oct})_3$) catalyzing reactions (Figure 1.5).

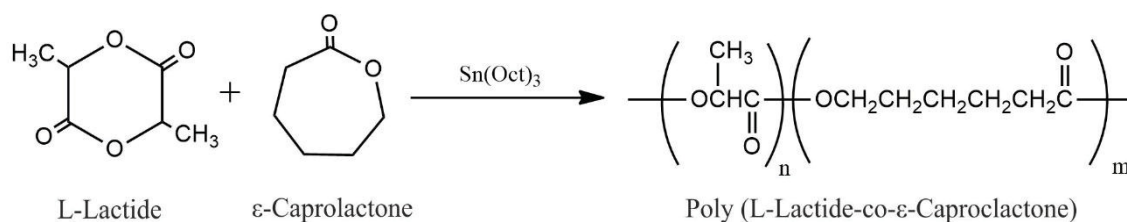


Figure 1.5. PLLCL synthesis from L-lactide and ϵ -caprolactone via $\text{Sn}(\text{Oct})_3$ catalyst.

It is a biodegradable, biocompatible, non-toxic and elastomeric co-polymer that widely used for cartilage,⁶⁸⁻⁶⁹ nerve⁷⁰ and cardiovascular regeneration.⁷¹ Mo et al. investigate biocompatibility of PLLCL 3D scaffold for tissue engineering applications.⁷² Influence of electrospinning parameters; polymer concentration and voltage were also investigated

for the formation of scaffolds and tissue engineering applications. Morphology of smooth muscle cells (SMC) and endothelial cells (EC) were examined according to their cellular behavior on nanofibrous structures. Thus, it was observed that the EC and SMC were proliferated and observed that characteristic morphology of EC was maintained. In another study, mechanical abilities of 3D PLLCL scaffold and its biocompatibility was investigated under varied circumstances (dry, wet and UV irradiated).⁷³ There was no obvious difference in mechanical characteristic in all conditions. Particularly, UV sterilization process did not damage the scaffold. Cell proliferation and viability trials were supported PLLCL scaffold and shown that it is a suitable material for skin tissue engineering applications. Recently, Laurent et al. were investigated PLLCL biocompatibility *in vitro* by using bone marrow mesenchymal stem cells (BM-MSC) and Wharton Jelly mesenchymal stem cells (WJ-MSC). Additionally, for *in vivo* applications a rat model was used for biocompatibility analysis.⁷⁴ In both circumstances, PLLCL scaffold were exhibited suitable properties for tissue engineering applications. Further, *in vitro* hydrolytic degradation results were showed that PLLCL scaffold became brittle which is a potential risk for anterior cruciate ligament tissue engineering (ACL). Therefore, mechanical strength might be a concern.

Besides good features of polyesters, they have some disadvantage as well. Biocompatibility of these polymer can be affected due to acidic degradation products.⁷⁵ These polymers tend to be stiff substances. Regarding to the aim, this property can provide benefits for load-bearing applications. In contrast, it is disadvantageous for soft tissues or blood vessels due to lack of mechanical strength. Also, polyesters, including other synthetic polymers do not show biocompatibility that facilitates cell attachment, proliferation and migration. Therefore, surface of the materials need to be functionalized with ECM proteins to provide cellular activities.

1.3.3. Composite Polymers

Natural and synthetic polymers have disadvantages where natural polymers are lack of mechanical strength, on the other side synthetic polymers cannot facilitate cellular activities. Therefore, scientists tried to overcome this problem by using composite (hybrid) scaffold to enhance mechanical and cellular features of the scaffolds by combining natural/synthetic materials.

Zhang et al. have fabricated PCL/Collagen nanofiber scaffold by using electrospinning technique.⁷⁶ Two different coating methods was applied by using collagen type I. One of them was forming a core shell other one was immersing PCL scaffold into collagen solution. These coated nanofibers were examined for biocompatibility analysis by using human dermal fibroblasts (HDF). The results indicated that HDF exhibit migration inside of core shell PCL-collagen scaffold. Moreover, core shell scaffold was showed higher proliferation compared to surface coated PCL-collagen scaffold that reform natural ECM. Rentsch et al. have fabricated PCL scaffold by melt spinning technique.⁷⁷ Collagen/chondroitin sulfate (coll I/cs) was used to coat the scaffold and examined the influence on calvaria bone regeneration *in vivo*. During six-month examination on bone formation, it was revealed that coll I/cs coated PCL improves the formation of the bone more than noncoated PCL scaffold. Based on histological and biomechanical analysis, it was proven as identical to autologous bone. In another related study, soft lithography technique was used to fabricate laminin (LN)-poly-D-lysine (PDL) substrate and neural stem cells behavior was investigated according to laminin distribution.⁷⁸ NSCs derived astrocytes migrated directly to LN strips rather than PDL but NSCs derived neurons did not migrate to LN strips. These results indicated that it can be further developed for nerve tissue engineering applications to study astrocyte and nerve interactions.

1.4. Scaffold Fabrication Techniques

Natural and synthetic biomaterials are used to producing 3D scaffolds that demonstrate structural and physiological similarities of natural ECM by varied biofabrication techniques. Therefore, a scaffold should show some properties such as mechanical strength, suitable pore size, high porosity to provide nutrient transport etc. Additionally, cell migration, proliferation, migration and spreading are affected from scaffolds properties as well. Some traditional fabrication techniques of 3D scaffolds are mentioned in the following section.

1.4.1. Solvent Casting/ Particle Leaching Method

Solvent casting is a very easy and inexpensive way to obtain a porous 3D scaffolds.⁷⁹ Instead of complex technological equipments or devices, it only depends on solvent evaporation processes. One of the major disadvantage is that removing toxic solvent from the membrane can cause denaturation of protein or can affect other solvents. Therefore, solvent casted membrane should be washed until toxic solvent is removed, and then needs to be dried under vacuum but this process is time consuming. To avoid these drawbacks, particle leaching is integrated with solvent casting, which provides uniform pore and size distribution (Figure 1.6).⁸⁰⁻⁸² Size of the pores can be adjusted according to concentration, size and shape of the particles such as salts, sugars, wax etc. In further process, after solvent evaporation only salt remain in the composite membrane. Then when it is immerse into water salt particles are leached to obtain a porous scaffold up to 500 μm (Figure 1.6).⁸³⁻⁸⁴

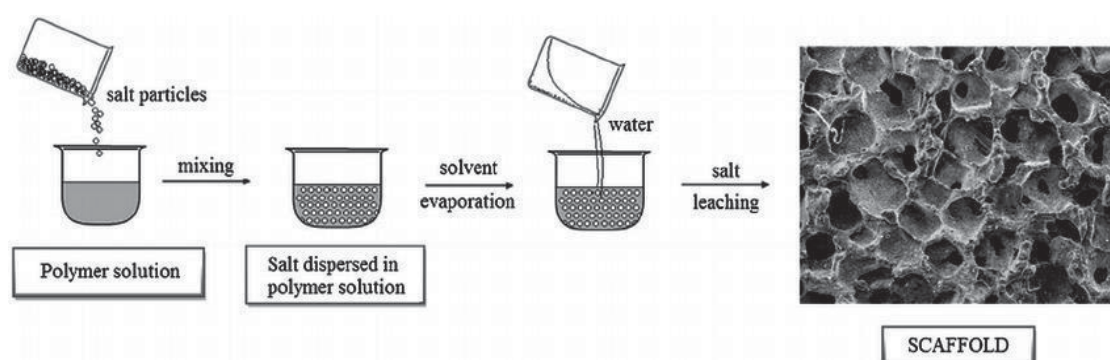


Figure 1.6. Schematic representation of solvent casting/particle leaching method.⁸⁵

1.4.2. Gas Foaming Method

In gas foaming carbon dioxide,⁸⁶ nitrogen⁸⁷ or water⁸⁸ are utilized as a foaming agents that is used at high pressures to form highly porous polymer scaffolds (Figure 1.7). Combination of gas molecules lead to nucleation due to thermodynamic driving forces and occurs gas bubbles within the polymer around 100-500 μm pore sizes. The amount and size of the porosity depends on the amount of gas that is dissolved in a polymer solution.⁸⁹

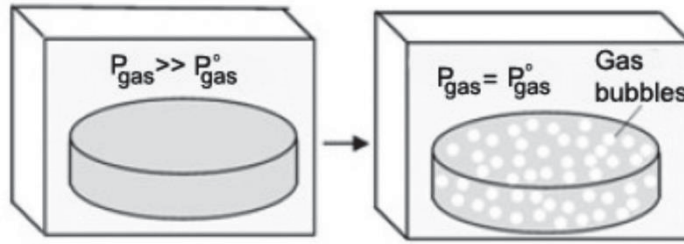


Figure 1.7. Scaffold fabrication by gas foaming technique.⁹⁰

The size of the pores and porosity can be adjusted with and without using porogen particles as particle leaching method. In this technique, inert gases are used that has not cytotoxic effect on cells. Limitation of this technique is that surface of the scaffold can be non-porous and within the scaffold large unconnected pores can be exist.⁹⁰

1.4.3. Freeze-Drying Method

Freeze drying, in other words lyophilization is another fabrication method to obtain porous 3D scaffold. In this method, biomaterials are dissolved to obtain a solution or a hydrogel form.⁸⁹ Then it is frozen below the freezing point of the materials and solvent solidifies into a crystal form (Figure 1.8). The solvent sublimates from the media under vacuum conditions, which form dry porous 3D scaffold. Pore formation is affected by polymer concentration, pH and size of the freeze solvent crystals. Freeze drying of a polymeric solution takes more time and high energy. Also, any solvent residue can influence cell viability.

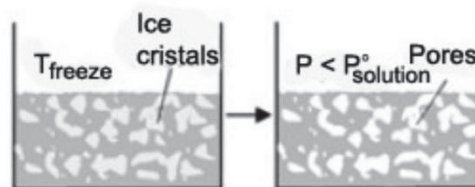


Figure 1.8. Schematic of freeze-drying method.⁹⁰

1.4.4. Rapid Prototyping Technique (RP)

Solid freeform fabrication (SFF) technique in other words rapid prototyping, is a new generation technology in tissue engineering fields.⁹⁰ Compared to other techniques, it is an advance 3D scaffold fabrication method. It is composed of computer control system (CAD) that provides internal and external shape control of scaffolds. Ceramics, metals, polymers are some of the materials that mainly used in RP. 3D structure of scaffolds are fabricated layer by layer via RP techniques including; electrospinning⁹¹⁻⁹², 3D printing,⁹³⁻⁹⁴ stereolithography,⁹⁵ selective laser sintering (SLS)⁹⁶ and fused deposition modeling (FDM)⁹⁷. Compared to other fabrication techniques, RP is more precise that can control the physical structure, biochemical abilities and degradation kinetic of the 3D matix.^{43, 98-99}

1.4.5. Electrospinning

The term of electrospinning originates by “electrostatic spinning” which was started to use around in 1994.⁹² The main idea of the system developed around 60 years ago where Formhals announce more than one patents.¹⁰⁰⁻¹⁰⁴ The equipments evolved in years, and it became more systematic, rapid, easy-to-use and versatile to fabricate nano-micrometer scales nanofibers.¹⁰⁵ Natural/ synthetic polymers, drug-nanoparticle integrated polymers, ceramics and composites are most widely used materials to obtain ultrathin fibers via electrospinning. This technique attracts more attention in scientific and industrial fields due to low cost, easy production, controllable pore size, large surface-to-volume ratio, high porosity and linked electrospun nanofibers.¹⁰⁵⁻¹⁰⁶ Because of these advantages, non-woven nanofibers mats were utilized in various field such as filtration,¹⁰⁷⁻¹⁰⁸ tissue engineering scaffolds,¹⁰⁹⁻¹¹⁰ drug delivery,¹¹¹ biomaterials for wound dressings¹¹¹⁻¹¹² biomedical and pharmaceutical applications.¹¹³⁻¹¹⁴

In tissue engineering, electrospinning technique is mainly preferred due to fibrillar structure and similarity of 3D microenvironment of natural ECM.¹¹⁰ Nanofiber scaffolds ensure high interconnected porous structure which provides nutrient transport, adhesion, proliferation, migration and differentiation of cells, so resulting in new form of tissue.^{5, 115}

The basic electrospinning system is represented in Figure 1.9. The system consists of four main parts; small diameter of needle (nozzle), solution pumping system, power supplier and grounded metal collector. Additionally, two electrodes of the system are attached to nozzle holder and metal collector. The polymer solution of the tip is held by its surface tension.¹⁰⁵

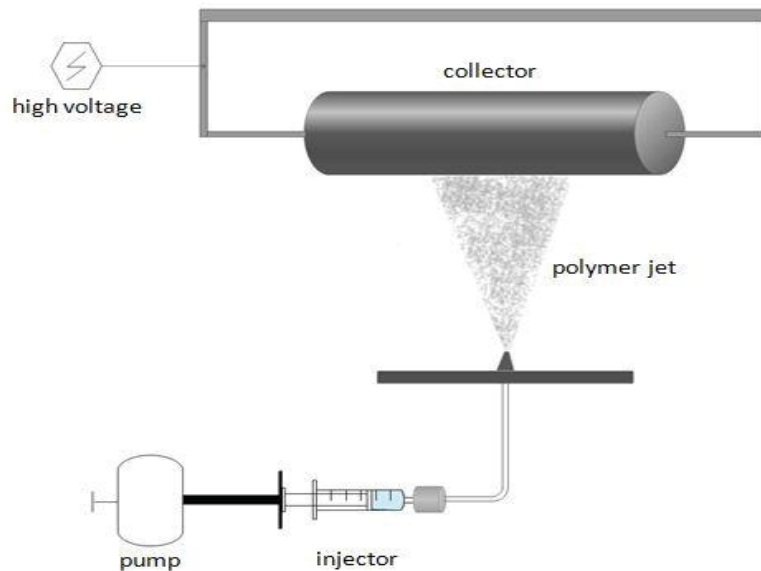


Figure 1.9. Schematic illustration of electrospinning system that composed of a pump system, syringe, conducting surface and power supply.

After applying high voltage, surface of the liquid is induced by electrical charges. Interaction between electrically charged polymer solution and electric field a droplet of conical structure is generated called as Taylor Cone where critical point of voltage is reached.¹¹⁶⁻¹¹⁷ At this point, electrical forces overcome surface tension, so solution can be ejected from the tip and charged jet solution can reach toward to collector, which have lower potential. While jet reaching to the conducting surface, solvent evaporate, and dry fibers accumulate on the ground collector at various sizes of fibers.

Electrospinning is influenced from electrostatic and viscoelastic behavior of solutions during nanofiber fabrication.¹¹⁸ Applied voltage, flow rate of solution, temperature, tip-collector distance, humidity is some of process parameters; solution concentration, molecular weight of material, conductivity, solvent vapor pressure,

surface tension, and viscosity mainly affect morphology and features of electrospun nanofibers.

Another type of electrospinning system is co-electrospinning technique. The working principle is the same as general spinning process. The only difference is that it is composed of two pump systems, two nozzle and syringes and two different solutions can be processed at the same time (Figure 1.10).

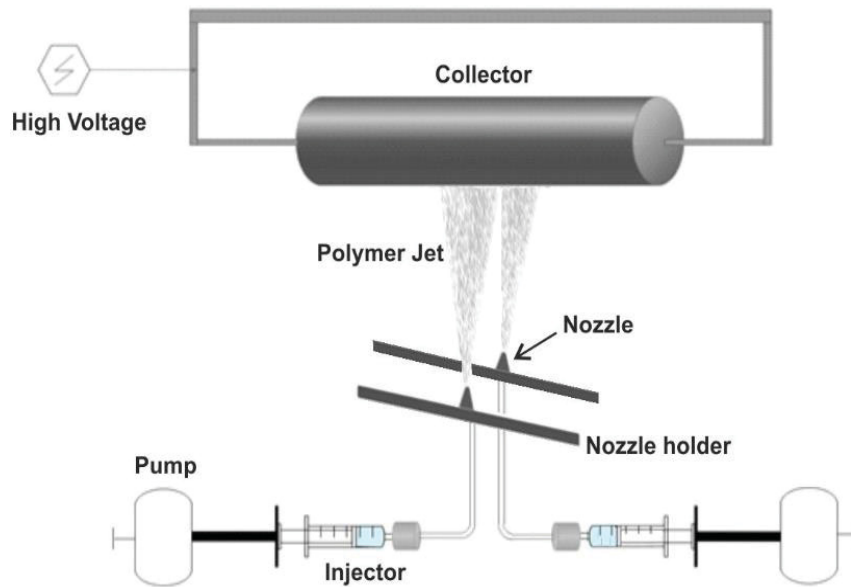


Figure 1.10. Schematic of co-electrospinning set up.

In the literature, the polymer materials were dissolved in same solvents, blended and subjected to electrospinning set up. All related studies which mentioned below were made by this concept. In one of the related study, PLLCL and collagen was dissolved in hexafluoro isopropanol (HFIP).¹¹⁹ By increasing collagen concentration, fiber diameter increases as well. Human umbilical vein endothelial cells (HUVEC) were seeded and they started to proliferate over high concentration of collagen/PLLCL scaffold. In another study, fibrinogen and PLLCL was dissolved in HFIP and blended in varied volume ratios.¹²⁰ Results supported the presence of fibrinogen within PLLCL. Moreover, HUVECs exhibited high viability and proliferation on fibrinogen/PLLCL blended scaffolds. Yin et al. were continued studying with collagen, chitosan and PLLCL materials that is blended with different ratios.¹²¹ PLLCL and collagen was dissolved in HFIP, chitosan was dissolved in HFIP and 2,2,2-trifluoroacetic acid (TFA). High content of collagen/PLLCL and low amount of chitosan scaffold showed the

highest mechanical strength. Compared to PLLCL scaffold, blended scaffold demonstrated higher endothelial cell viability which makes it a good candidate for vascular graft applications. A sandwich model collagen/ PLLCL scaffold were also investigated for cartilage tissue engineering.¹²² Both materials were dissolved in HFIP and mixed at equal proportions. One sheet of scaffold was seeded with chondrocytes and covered with another sheet and same amount of cell was seeded till 20 sheet stacked scaffold was obtained. *In vivo* applications showed that cartilage formed tissue was observed after 8 weeks of implantation. Mechanical strength was increased like native cartilage tissue in 12 weeks. The results indicated that collagen/ PLLCL scaffold is a suitable scaffold for cartilage tissue engineering applications. All these studies have a common point; collagen was dissolved in HFIP which is a very toxic, non-biocompatible and mostly not preferred for biological applications. Therefore, in this study, co-electrospinning method was developed and collagen containing PLLCL scaffolds were fabricated successfully while avoiding heavy chemicals.

CHAPTER 2

MATERIALS AND METHODS

2.1. Materials

Poly (L-lactide-co- ϵ -caprolactone) (PLLCL, Resomer, Evonik Industries), polyvinylpyrrolidone (PVP, average M_w 360,000, Sigma Aldrich) and polyvinyl alcohol (PVA, average M_w 30,000-70,000 Sigma Aldrich) were used for fabrication of polymer scaffolds. Dimethylformamide (DMF, $\geq 99\%$, Sigma Aldrich), dichloromethane (DCM, $\geq 99\%$, Sigma Aldrich) and deionized water were used to dissolve polymers. Type I Collagen from calfskin purchased from Sigma Aldrich. Acetic acid ($\geq 99\%$, Sigma Aldrich) was used to dissolve collagen. Lysozyme from chicken egg white in the form of lyophilized powder ($\geq 90\%$, $\geq 40,000$ units/mg protein, Sigma Aldrich) was used for enzymatic biodegradation studies. BCA protein kit (Bicinchoninic Acid, Pierce Thermo) and BSA as lyophilized powder (Bovine serum albumin, Sigma Aldrich) were used for protein adsorption analysis. 1X phosphate buffer saline (PBS, pH 7.4 Gibco-Thermo Fischer) was used for hydrolytic biodegradation as well as cleaning and solubilizing agent. Sodium dodecyl sulfate (SDS, Bioshop), Tween80 (Bioshop), Tween 20 (Bioshop) and Triton X-100 (Bioshop) were used for protein adsorption analysis. Anti-Collagen Type I-FITC Antibody was purchased from Merck and used for collagen immunostaining of scaffolds. For cell culture analysis; NIH-3T3 mouse fibroblast cell line (ATCC® CRL-1658™), Dulbeccos Modified Eagle's Medium (DMEM high glucose, Sigma Aldrich), fetal bovine serum (FBS-Gibco), penicillin-streptomycin (Sigma Aldrich), trypsin EDTA solution (Sigma Aldrich) were used for cell culture studies. Dimethylsulphoxide (DMSO, Carlo Erba) was purchased. *In vitro* cell proliferation, cytotoxicity and viability was analyzed with resazurin sodium salt from ChemCruz, MTT (3-(4, 5-dimethylthiazolyl-2)-2,5-diphenyltetrazolium bromide) from Sigma Aldrich and CytoCalcein AM and Propidium Iodide dye (AAT Bioquest) used for live/dead assay.

2.2 Methods

2.2.1. Fabrication of PLLCL Scaffold

Poly (L-lactide-co- ϵ -caprolactone) (PLLCL) scaffold was fabricated by electrospinning technique. 1,435 g PLLCL (10wt %) was weighed in 20 mL vial and dissolved in 9 mL of DCM and 1 mL of DMF solvent mixture and mixed on magnetic stirrer for one day. After PLLCL completely dissolved, 20 mL syringe was filled with polymer solution and connected to syringe pump of the electrospinning set up (Figure 2.1). The collector coated with aluminum foil. Electrospinning parameters were adjusted as indicated; 25kV voltage, 3mL/h flow rate, 180 mm tip collector distance, homogeneity mode of collector and rotation are turned on. After PLLCL collected on the aluminum foil, was dried at room temperature and stored at +4°C.



Figure 2.1. Electrospinning device (Inovenso NE300)

2.2.2. Fabrication of PLLCL/PVA/Collagen and PLLCL/PVP/Collagen Scaffolds

1.25 g of PVA (20%wt) was weighed in 20 mL vial, dissolved in 5mL deionized water and stirred overnight on magnetic stirrer. 16 mg of collagen (0.4%) was dissolved in 1.5 mL, 0.1M acetic acid by continuous stirring for 3 hours. After 3 hours, 2.5 mL

PVA is added over collagen solution and mixed for an additional hour on magnetic stirrer. Then 20 mL syringe was filled with PVA/ Collagen solution and placed in the electrospinning setup. Co-electrospinning was applied by using two pump systems and two nozzles (Figure 2.2). Electrospinning parameters were adjusted for PVA/Collagen as indicated; 2 mL/h flow rate, 30 kV and 150 mm, for PLLCL is 3mL/h flow rate, 30 kV and 150 mm. Collected polymer scaffolds were stored at -20°C. SEM images were taken to observe the fiber formation and to compare the presence and absence of PVA. To obtain PLLCL/0.4%Collagen, scaffold immersed into deionized water for 2 days to remove PVA and allowed to dry at room conditions.

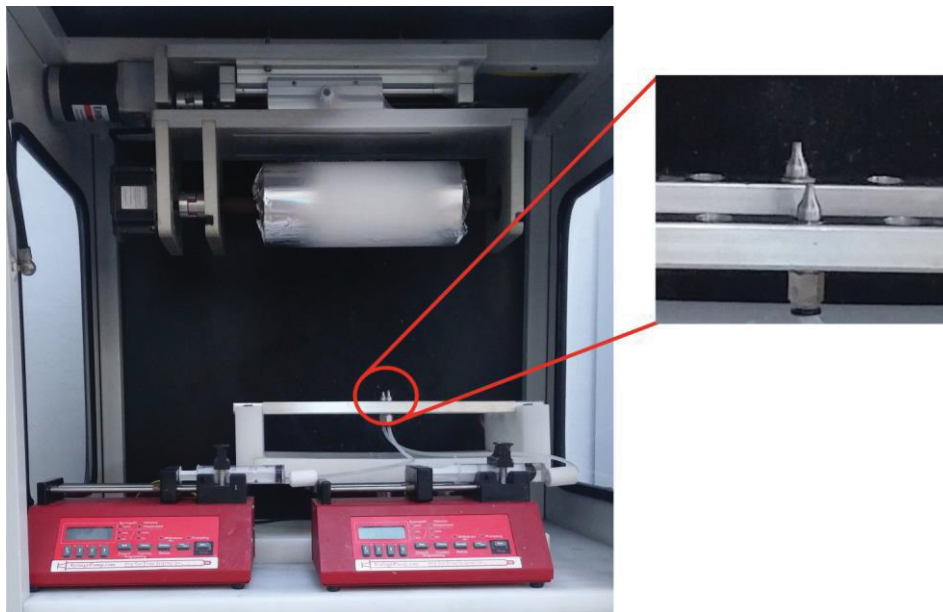


Figure 2.2. Co-electrospinning set up with two nozzles and two pump systems.

When PVP is used as a carrier agent 2.5g PVP (20%wt) was weighed in 20 mL vial, dissolved in 10 mL deionized water and mixed overnight on stirrer. Either 20 mg collagen (0.4 %w/v) or 40 mg collagen (0.8% w/v) was dissolved in 1.5mL 0.1M acetic acid for 1 hour. 3.5 mL 20% PVP added over each collagen solution and completed to 5mL. Prepared PVP/Collagen solution was used for co-electrospun with PLLCL solution. PVP/Collagen parameters arranged to 3mL/h flow rate, 120 mm distance and 30 kV voltage was applied. The flow rate of PLLCL was constant at 3mL/h, distance and voltage arranged according to PVP/ collagen solutions.

For 1% Collagen, 50mg collagen (1% w/v) dissolved in 2mL of 0.1M acetic acid for 3 hours then mixed with 3mL of 15%wt PVP for another hour. Due to high viscosity

of collagen, the concentration of PVP was reduced to 15%wt (0.75g) and dissolved in 5mL deionized water, then stirred overnight. Co-electrospinning was done at 2.5mL/h flow rate, 105 mm and 30kV for PVP/1%Collagen solution with 3mL/h flow rate of PLLCL. Further, PVP was removed from the scaffold by immersing into deionized water for 2 days and allowed to dry at room conditions. PLLCL/0.4%Collagen, PLLCL/0.8%Collagen and PLLCL/1%Collagen stored at -20°C to prevent denaturation of collagen.

For characterization and further analysis steps, PLLCL/PVA and PLLCL/PVP scaffolds were separately fabricated with fixed polymer concentrations; 20% of PVA, 20% PVP and 10% of PLLCL to compare the effect of collagen on the scaffolds.

2.2.3. Characterization Tests

2.2.3.1. Scanning Electron Microscope (SEM) Analysis

Surface homogeneity of scaffolds, porosity and diameter was analyzed via scanning electron microscope (SEM- Quanta FEG 250) by using Image J Software (NIH). Scaffolds were cut and fixed on carbon bands and coated with thin gold layer under argon gas (Emitech K550X). Scaffolds were analyzed in varied magnifications.

2.2.3.2. Collagen Immunostaining Analysis

Collagen Type I-FITC Antibody was used to detect collagen type I presence in scaffolds and illustrated under fluorescence microscope. PLLCL, PLLCL/PVP, PLLCL/PVP/0.8%Collagen, PLLCL/0.8%Collagen (after removing PVP), PLLCL/PVP/1% Collagen, and PLLCL/1%Collagen (after removing PVP) scaffolds were cut in round shapes and fit in a 96 well plate as three replicates. To prevent non-specific binding of antibodies 1% BSA solution was used as blocking agent, which is prepared in 1X PBS, and 50 μ L of BSA solution was added on each scaffold and incubated one day. Anti-collagen type I antibody and 0.5% BSA mixed to 1:100 volume ratio and stirred gently. 50 μ L added on scaffolds and covered with aluminum foil.

After overnight incubation at room temperature, scaffolds washed with 1X PBS three times. Fluorescence microscope was used to imaging collagen on scaffolds (Zeiss Observer Z1).

2.2.3.3. Fourier Transform Infrared - Attenuated Total Reflectance Spectroscopy (FTIR-ATR) Analysis

FTIR analysis was performed to identify the presence or absence of PLLCL, PVA, PVP and collagen on the scaffolds. Molecular investigation of scaffolds was done by using Perkin Elmer model FTIR-ATR instrument that has diamond/ZnSe crystal. Scaffolds were compared with pristine PLLCL, Collagen, PVA and PVP. Fabricated scaffolds were placed on the crystal and compacted with the pressure arm and scanned. Scanning was applied between 650 - 4000 cm^{-1} wavenumber range with a resolution rate of 4 cm^{-1} and scan number of 20. The obtained data was plotted using graphing software OriginPro (Northampton, MA).

2.2.3.4. Contact Angle Analysis

Water contact angle measurements provide information about surface hydrophilicity of scaffolds. Distilled water used as a reference liquid. The instrument (Attension) that was used in this analysis was used in manual mode and the droplet size was set to 5 μL . PLLCL, PLLCL/PVA, PLLCL/PVA/0.4%Collagen, PLLCL/0.4%Collagen (after removing PVA), PLLCL/PVP/0.4% Collagen, PLLCL/0.4%Collagen (after removing PVP), PLLCL/PVP/0.8% Collagen, PLLCL/0.8%Collagen (after removing PVP), PLLCL/PVP/1% Collagen, and PLLCL/1%Collagen (after removing PVP) were fixed separately on glass lam by using double side adhesive bands to obtain smooth surface. The angle between water drop and surface of the scaffold were measured for five different points of PLLCL, PLLCL/PVP/Collagen and PLLCL/Collagen scaffolds and the average value was evaluated.

2.2.3.5. Protein Adsorption Assay

Protein adsorption assay was made with the bicinchoninic acid (BCA) assay which determine total adsorbed protein amount on scaffold surfaces. According to the instruction of the kit; 4 mg of BSA dissolved in 2mL 1X PBS which was prepared as a stock solution (for each scaffold stock renewed). Dilution series were prepared according to table 2.1 at specific concentration range of BSA samples.

Table 2.1. Bovine serum albumin (BSA) standards preparation

Test Tubes	Volume of 1X PBS (μL)	Volume of Source of BSA (μL)	Final BSA Concentration (μg/mL)
A	0	300 of Stock	2000
B	125	375 of Stock	1500
C	325	325 of Stock	1000
D	175	175 of test tube B dilution	750
E	325	325 of test tube C dilution	500
F	325	325 of test tube E dilution	250
G	325	325 of test tube F dilution	125
H	400	100 of test tube G dilution	25
I	400	0	0

PLLCL, PLLCL/PVA, PLLCL/PVA/0.4%Collagen, PLLCL/PVP, PLLCL/PVP/0.8%Collagen and PLLCL/PVP/1%Collagen scaffolds were cut into 6 mm diameter of round shapes and placed in 96 well plate. For each concentration 3 replications were prepared. Before the adsorption study, PLLCL was incubated with 1X PBS for one day. Following day, PLLCL scaffolds were taken from PBS and placed into clean wells. 25 μL of each BSA solution was separated to measure the initial solution without scaffolds. 50 μL from each BSA solution was added into another 96 well plate, scaffolds immersed in it and incubated for 2 hours at 37 °C. After 2 hours, 25 μL of solutions were taken to measure final concentrations. At the same time scaffolds were removed from solutions and washed three times in 1X PBS. Then immersed into 50 μL of 5% detergent solution (Tween 80, Tween 20, TritonX-100,

SDS) and incubated 1 hour at 37 °C. 25 µL of these solutions were analyzed as detergent solubilized samples. At the end of the experiment three type of samples were obtained named initial, final and solubilized protein samples. Working reagent (WR) of the kit containing cupric sulfate and in alkaline medium where Cu^{+2} was reduced to Cu^{+1} in the presence of protein and BCA make a chelate with cuprous ion. This chelate gives the purple colored solution and a strong absorbance at 562 nm. Sample to WR ratio needs to be in 1:8 ratio. At the first stage 25 µL of samples were taken, so 200 µL of WR needed for the reaction. WR is prepared according to the number of working wells. After addition of 200 µL of WR to unknown samples (initial, final, solubilized proteins concentration), solutions were covered aluminum foil and incubated 30 min at 37 °C. From high concentration to low concentration, the color changes from dark to clear purple. After that solutions cooled to room temperature, the absorbance was measured at 562 nm for each well on a plate reader (Fisher Scientific™ accuSkan™ GO UV/Vis Microplate Spectrophotometer). The experiment repeated for Tween80, Tween20, TritonX-100, SDS to see solubilizing effects of detergents.

2.2.3.6. Mechanical Analysis

Mechanical strength of PLLCL, PLLCL/PVP, PLLCL/PVP/0.8%Collagen, PLLCL/0.8%Collagen (after removing PVP), PLLCL/ PVP/ 1% Collagen, and PLLCL/ 1% Collagen (after removing PVP) scaffolds were measured by tensile test method. The tensile specimen platform (dog bone) was made of polymethylmethacrylate (PMMA) which obtained by laser ablation (Epilog Zinc) technique. All samples were cut in dog bone shape as four replicates. Cross-sectional images were taking from scaffolds by using SEM, and average thickness was calculated via Image J (NIH) software. Tensile test was performed by using TA. XT Plus Texture Analyzer (Stable Micro Systems) with an elongation speed of 20 mm/min. By leaving 4.5 cm gauge length for mechanical loading, the end of the square specimens mounted on two 15mm x 15mm gripping units of the tensile tester. Stress-strain curves were obtained from the electrospun scaffolds. Depending on strain stress curve, young modulus, ultimate tensile strength was calculated.

2.2.3.7. Hydrolytic and Enzymatic Biodegradation Study

Biodegradation behavior of scaffolds was made observed in hydrolytic and enzymatic conditions. For 20 weeks biodegradation experiments, scaffolds were cut into 1.0x1.0cm² squares for hydrolytic degradation, and 1.5x1.5cm² squares for enzymatic degradation. Weighed samples were soaked into 1X PBS while other group of samples soaked into 1.5 µg/mL of lysozyme solution. Both groups were incubated at 37°C with constant shaking at 240 rpm for 20 weeks by using Thermo Shaker MS100. Incubation solutions were renewed each week. Every analysis week, scaffolds were washed with deionized water three times and put in desiccator to dry completely. Before scaffolds were drying, wet weights of samples were recorded and were put in desiccator until completely drying. Weight loss of the samples calculated regarding to following equation where W_0 is weight of scaffold before biodegradation, W_t is dry weight after biodegradation;

$$\text{Weight loss (\%)} = \frac{W_0 - W_t}{W_0} \times 100$$

After scaffolds completely dried, morphological changes was also examined with SEM.

2.2.3.8. *In vitro* Cell Culture Studies

Fresh culture medium was prepared each time prior to use. For 500 mL complete medium, 420mL DMEM (high glucose), 75 mL FBS (15%) and 5mL streptomycin and penicillin (1%) was mixed gently and stored at +4°C. Before using complete medium, it was heated in water bath at 37°C. Frozen NIH3T3 mouse fibroblast cell stock taken from -80 °C and dissolved in water bath. Dissolved cells were slowly added in 10mL, 15% complete medium and centrifuged for 5 min at 1000 rpm. Supernatant was removed, and precipitated cells were resuspended in 1 mL 15% medium. Then it was added in 25 cm² cell culture flask and completed with 5 mL 15% complete medium. Cells were incubated under 5% CO₂ at 37°C while cells reach to 80-90% confluency, and then they were harvested and passaged to 75 cm² cell culture flask. Cells were expanded until reaching desired cell number for further experimental steps.

2.2.3.8.1. Cell Seeding on PLLCL/Collagen Scaffolds

Trypsin-EDTA solution from -20°C, 10% complete medium and 1X PBS was taken from +4°C and heated in water bath at 37°C. 75 cm² cell culture flask was taken from the incubator and complete medium was discarded. 5mL of 1X PBS was added and washed to remove remaining medium to prevent inhibition of trypsin-EDTA activity. PBS was discarded from the flask, 3mL trypsin-EDTA solution was added for 3 min incubation. Trypsin activity was inhibited by adding complete medium and remaining solution centrifuged at 1000rpm for 5 min. Then supernatant was discarded, and precipitated cells were suspended in 1mL cell medium. For cell counting, resuspended cells were diluted to 1:10 ratio with cell medium and trypan blue. 10μL of solution was loaded in hemocytometer and counted.

Scaffolds were cut in round shape to fit in 96 well plate. Sterilization was applied under ultraviolet light (UV-245nm) for 30 min for each side. PLLCL/PVA/0.4%Collagen, PLLCL/PVP/0.8%Collagen and PLLCL/PVP/1%Collagen scaffolds were immersed in deionized water for 2 days with continuous shaking to remove the carrier materials or namely sacrifice polymers; PVA and PVP. Each scaffold placed in 96 well plate as 3 replicates. 10000cell/per well seeded over scaffolds with 10% complete medium and incubated in 5% CO₂ at 37°C overnight. After overnight incubation, scaffolds were taken from the complete medium and transferred to clean wells with a 100 μL complete medium to avoid false measurement due to excess adhesion of cells to the well surface.

2.2.3.8.2. Cell Proliferation and Viability on PLLCL/Collagen Scaffolds

Cells proliferation on scaffolds was investigated for short-term cell culture studies utilizing NIH3T3 cells. Short-term analysis was performed for 1. / 3./ 5. and 7 days, where 10000 cells/per wells were seeded on scaffolds. MTT assay was used to measure proliferation, viability and cytotoxicity of cells on scaffolds. It is a colorimetric method, where yellow tetrazolium bromide is metabolized in mitochondria from viable cells and reduces into purple formazan crystals. Dark purple related to higher viable cells, in contrast, light purple shows lower viable cells. Therefore, cell viability is

validated depending on the color and absorbance change. In other colorimetric method, a blue non-fluorescent resazurin reagent is used which is alamar blue assay. It is a fluorometric analysis, which can be also used for absorbance analysis to examine proliferation profile of cells on scaffolds. Blue resazurin, metabolites by viable cells into resorufin and change the culture media to pink. As the number of viable cell number increased, proportionally resorufin production increases as well. Final concentration of alamar blue was 0.01% where 1mL alamar blue and 99mL complete medium was added over scaffolds. Complete medium including alamar blue was used as a blank and incubated for 2-4 hours. After incubation, solutions were transferred into clean wells and measured at 570-600nm by using microplate reader. Proliferation percentage of viable cells were calculated based on absorbance values.

Cell viability was also determined by live/dead assay, which gives the exact proportion of live/dead cells through fluorescence microscopy images. To conduct the live/dead assay on scaffolds, propidium iodide (PI) and CytoCalcein™ Green was added at equal proportions in buffer solution. Complete medium of cell seeded scaffolds was replaced with 25 µL of fresh cell medium and 25 µL live/dead solution, then incubated for 30 min at 37°C. Then scaffolds were and transferred to clean wells for further washing steps. Each side of scaffolds was examined by fluorescence microscope (Zeiss Observer Z1).

2.2.3.8.3. Morphological Analysis of Cell Proliferations on PLLCL/Collagen Scaffolds

NIH3T3 cells were seeded in 96 well plate as 2500cell/ well for 1, 3, 5 and 7day cell culture periods. After incubation, scaffolds were washed three times with 1X PBS. Then 50µL of 4% paraformaldehyde added over scaffolds and incubated for 1 hour at 37°C. Then, paraformaldehyde solution was discarded, and scaffolds were washed three times with 1X PBS. Scaffolds were dried in desiccator. Dried scaffolds were fixed on carbon bands and coated with thin gold layer to increase conductivity of samples. Finally, scaffolds were characterized via SEM at varied magnifications.

CHAPTER 3

RESULT AND DISCUSSION

3.1. Characterization of PLLCL Nanofibers

Optimization studies have been carried out to control the morphology of PLLCL scaffold. First, optimum solvent type and ratio was determined. In this aspect, DCM and DMF solvents were used to solubilize 10% PLLCL. While increasing the amount of DMF from 0.5mL to 2.5 mL and decreasing DCM from 4.5mL to 2.5mL, solubility of PLLCL decreased, and solution became turbid. For these solvent ratios, electrospinning was applied but fiber formation was not observed. Due to high surface tension of DMF,¹²³ its cannot exceeded by electric field and prevents jet formation. In contrast, if the amount of DCM increased from 2.5mL to 4.5 mL while decreasing DMF from 2.5mL to 0.5mL solubility of PLLCL increased and solution became transparent (Figure 3.1). Owing to rapid evaporation of DCM phase separation occurs, so during the electrospinning pores are formed on the surface of the fibers. Also, only DCM was used to solubilize PLLCL but because of its low boiling point and high evaporation rate, polymer solution frozen on the tip. According to these findings, optimized solvent mixture ratio was 4.5:0.5 (DCM: DMF) to solubilize the PLLCL without heating.

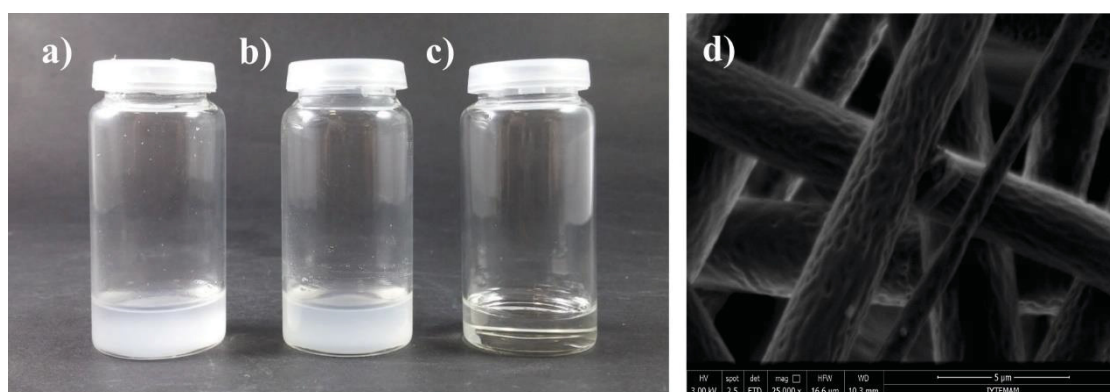


Figure 3.1. Solutions of PLLCL in varied DCM: DMF ratio, a) 2.5:2.5 mL, b) 3.5:1.5 mL and c) 4.5:0.5 mL, d) SEM micrograph of porous PLLCL fiber in 4.5:0.5 mL DCM: DMF.

Once the appropriate solvent ratio has been determined, experiments were performed at different PLLCL concentration that affects directly the fiber morphology. 5%, 8%, and 10%wt PLLCL solutions were prepared in 4.5:0.5mL DCM: DMF at different electrospinning parameters until fiber formation is observed. No fiber formation was observed under 5% due to lack of chain entanglement between polymer chains. Also, low surface tension, low viscosity and low conductivity of polymer solution resulted in breaking up jets and forming beads. Even if by increasing concentration from 5% to 8%, elongated or stretched beads were formed which shows the jet is still not stable enough (Figure 3.2a-b).

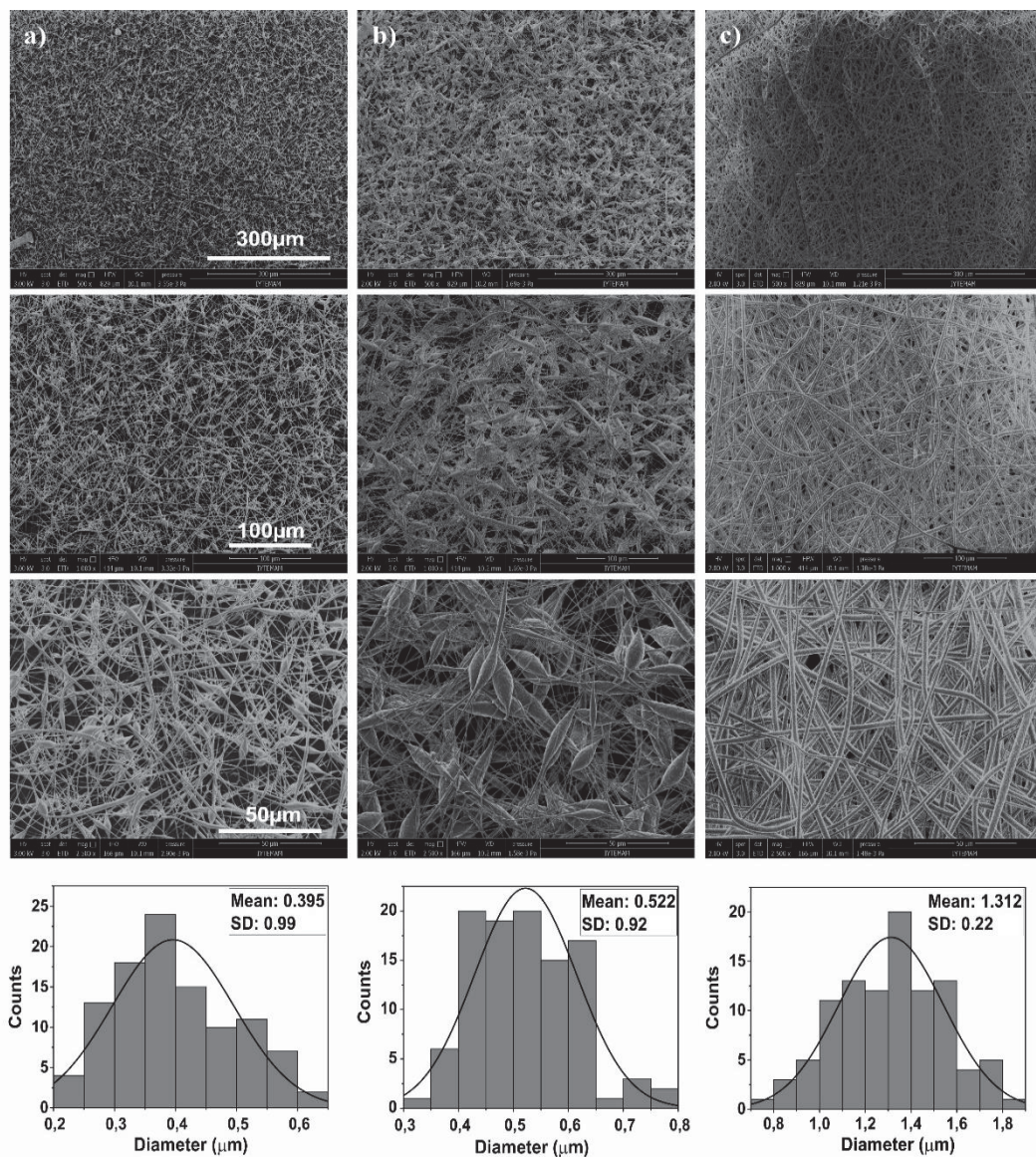


Figure 3.2. SEM images of electrospun PLLCL scaffolds and fiber distribution in varied concentration of PLLCL a) 5%wt, b) 8%wt and c) 10%wt.

Distance between elongated beads decreased with increasing concentration of PLLCL solution, which shows that chain entanglement among polymer chains increased slowly to form nanofibers. When 10% PLLCL solution was used, viscosity of the solution reached to optimum level, which overcome the surface tension, so polymer solution can easily go through the electric field to form uniform, homogeneous fibers at the collector (Figure 3.2c).

Figure 3.2 shows SEM analysis and diameter distribution of PLLCL fibers in varied polymer concentrations at a constant flow rate 3mL/h. Also, distance and voltage have been adjusted with only small differences, but they were not as much effective parameters as concentration itself. Fiber diameters of 5% and 8% PLLCL was observed as $0.395 \pm 0.99\mu\text{m}$ and $0.522 \pm 0.92\mu\text{m}$. The decrease in the number of beads indicates that fiber formation has taken place. Homogeneous fiber formation is obviously seen at 10% PLLCL which has average diameter of $1.312 \pm 0.22\mu\text{m}$. In literature, it was also shown that the fiber diameter changed depending on the polymer concentration. As the concentration increases, the fiber diameter increases, and the pore size decreases.¹²⁴⁻¹²⁶

While optimizing the concentration of PLLCL, electrospinning parameter was optimized as following; 3 mL/h of flow rate, 25kV voltage and 18 cm tip to collector distance. In further studies, optimized parameters were used to fabricate nanofiber membranes for other analysis steps.

3.2. Characterization of PLLCL/ Collagen Scaffolds

In literature, collagen was dissolved in HFIP and electrospun with or without polymer materials.^{119, 127-130} Especially for biological applications like tissue engineering and 3D cell culture, instead of toxic chemicals, non-toxic chemicals and solvents, if possible water-based systems should be preferred. Therefore, in this work acetic acid solution was utilized as a solvent, which is less harmful compared to HFIP. In the first trial collagen dissolved in 0.1M acetic acid and mixed in 10% PLLCL. While adding collagen solution in PLLCL, it started to precipitate. Even at high rpm, complete solubilization was not obtained and collagen was dispersed in PLLCL solution. The reason can be explained with polarity differences; where DCM (polarity index: 3.1) and acetic acid (polarity index:6.2) are not miscible due to their polarity differences. To overcome this problem, a new methodology has been developed by utilizing a “water

soluble” polymer; namely PVA and PVP as a co-electrospinning or sacrificing agents. Here, either PVA or PVP solutions were used as a helping reagent which prevents precipitation of collagen and facilitates it electrospinning. Since both co-electrospinning agents, PVA and PVP, are water-soluble so they can be removed from the polymer scaffold easily by solubilizing them with water. Therefore, they behave as sacrificing agent. Prior to polymer scaffold fabrication, either PVA or PVP was solubilized with distilled water and washed away to obtain PLLCL/Collagen scaffold.

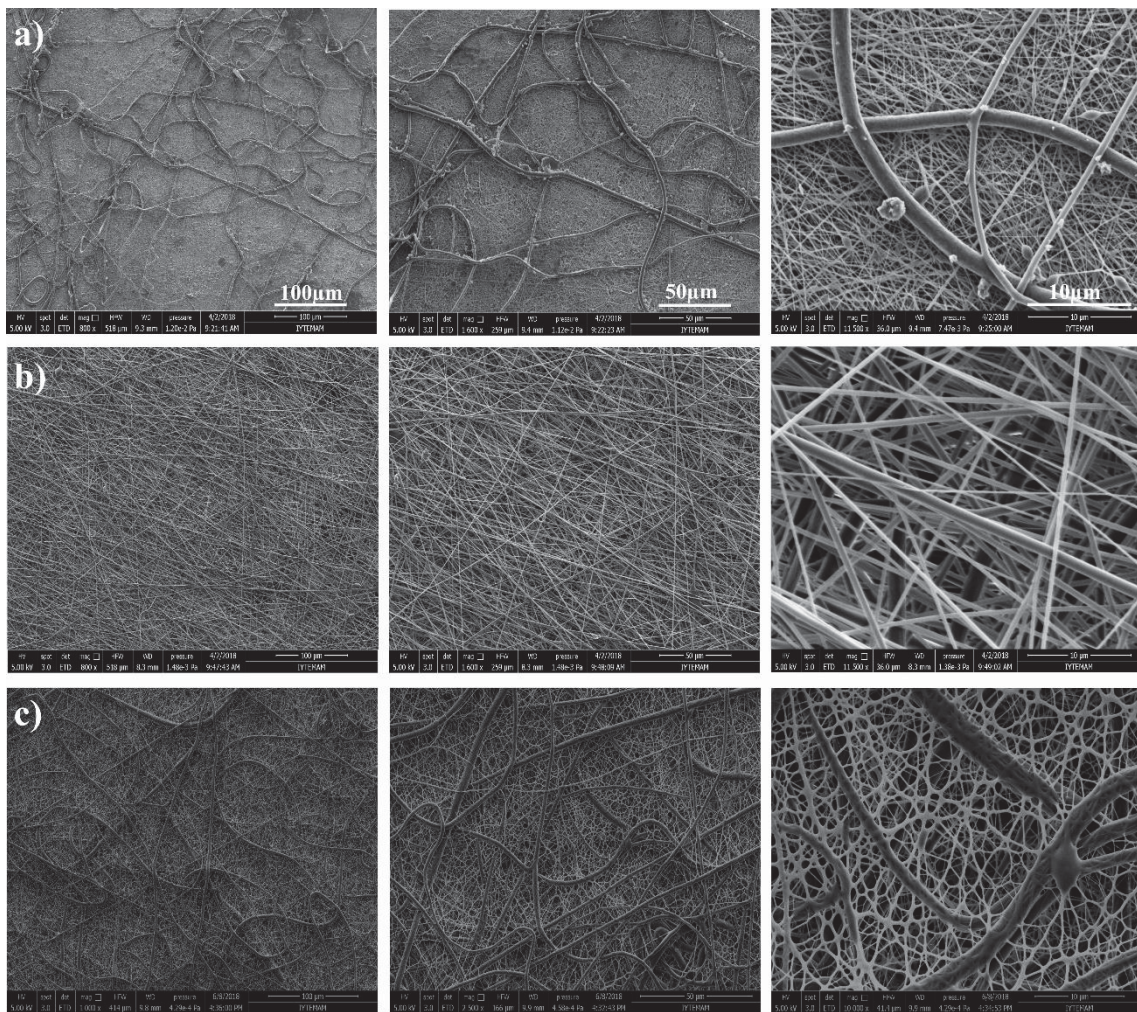


Figure 3.3. SEM micrographs of co-electrospun scaffolds right after spinning (without washing with deionized water), a) PLLCL/PVA/0.4%Collagen, b) PLLCL/PVP/0.8%Collagen and c) PLLCL/PVP/1%Collagen.

Following solutions were prepared separately; 0.4%w/v collagen mixed with 20% PVA, 0.8%w/v with 20%PVP and 1%w/v of collagen mixed with 15% PVP and co-electrospun with PLLCL solution as explained in detail at section 2.2.2. Only flow rate was different due to viscosity differences; 3mL/h for PLLCL, 2mL/h for PVA/

Collagen and 3-4mL/h for PVP/ Collagen. The applied voltage 30kV and tip-collector distance changes depending on co-electrospinning agents. Prior to scaffold fabrication and sacrificing agent removal, morphological characteristics of scaffolds were evaluated through SEM analysis. In figure 3.3, morphological differences between PLLCL, PVA and PVP can be easily noticed. PVA and PVP have thinner diameter fibers which can be easily differentiated from thicker fibers of PLLCL. The diameter of PVA and PVP does not have a significant effect since they are sacrificed after co-spinning of collagen. Moreover, PLLCL/PVA/0.4%Collagen, PLLCL/PVP/0.8%Collagen and PLLCL/PVP/1% Collagen scaffolds immersed into water to solubilize and wash away either PVA or PVP from the scaffold. The removal of PVA or PVP was confirmed via SEM images (Figure 3.3) which only thick fibers were remained. Finally, only collagen containing PLLCL scaffold remained which was the major scaffold of this study (Figure 3.4).

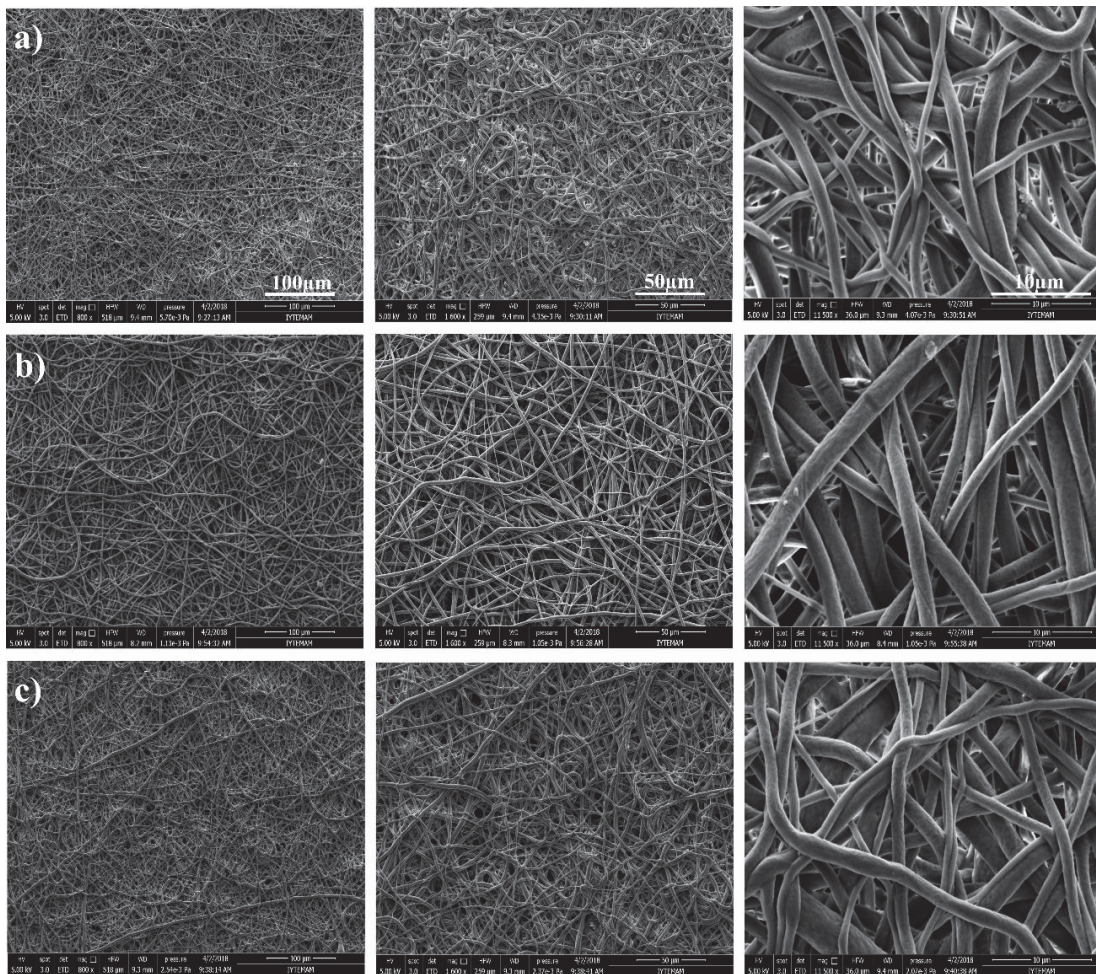


Figure 3.4. SEM micrographs of co-electrospun scaffolds prior to removal of sacrificing agents (after washing with deionized water), a) PLLCL/0.4%Collagen, b) PLLCL/0.8%Collagen and c) PLLCL/1%Collagen.

3.3. Immunostaining of PLLCL/Collagen Scaffolds

The immunostaining analysis was performed to identify collagen on PLLCL scaffolds with and without PVP. For immunostaining, monoclonal IgG1 conjugated to FITC antibody against collagen was used to observe collagen under fluorescence microscope. Depending on nanofiber formation collagen grafting changes. In figure 3.5a-b, there is no fluorescence signal observed from PLLCL and PLLCL/PVP scaffolds, but PLLCL/PVP/0.8%Collagen (Figure 3.5.c) and PLLCL/PVP/1%Collagen (Figure 3.5e) scaffolds there is a strong fluorescence signal which indicates presence of collagen in the polymer scaffolds. Even after removal of PVP, fluorescence signal remains that clearly indicates the presence of collagen in PLLCL scaffolds (Figure 3.5d, f).

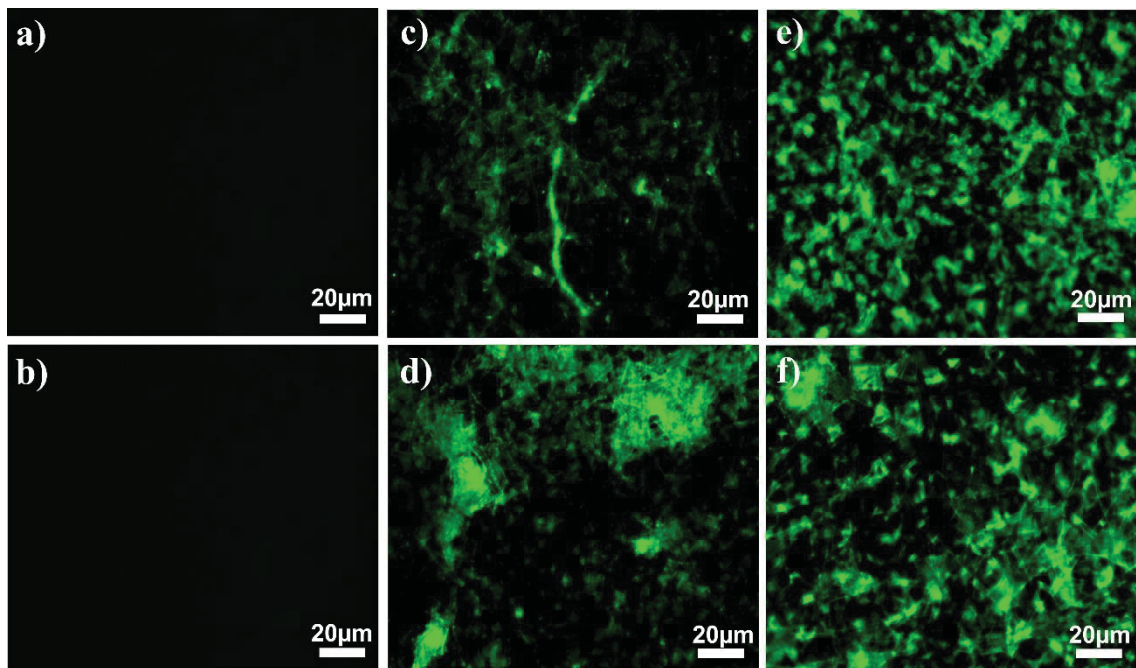


Figure 3.5. Fluorescence microscopy images of immunostained scaffolds, a) PLLCL, b) PLLCL/PVP, c) PLLCL/PVP/0.8%Collagen, d) PLLCL/0.8%Collagen (after removing PVP), e) PLLCL/PVP/1%Collagen, and f) PLLCL/1%Collagen (after removing PVP).

3.4. FTIR-ATR Analysis of PLLCL/Collagen Scaffolds

The FTIR spectra of pristine Collagen, PLLCL, PVP, PVA were shown in figure 3.6, PLLCL/PVA/0.4%Collagen and PLLCL/0.4%Collagen after PVA removal were shown in figure 3.7, PLLCL/PVP/0.8%Collagen, PLLCL/0.8%Collagen, PLLCL/PVP/1%Collagen and PLLCL/1%Collagen after PVP removal were shown in figure 3.8. Collagen type I has characteristic peaks at 1636 cm^{-1} , 1550 cm^{-1} and at 1240 cm^{-1} which corresponds to amide I, amide II and amide III bands. Amide I belong to the C=O group in the polypeptide backbone which shows stretching vibrations from 1600 to 1700 cm^{-1} . Amide II band demonstrates vibration of the N-H bending and amide III band demonstrate C-H stretching vibrations. Hydrogen bonded N-H group of peptides was found at 3320 cm^{-1} . While examining PLLCL spectrum, a sharp peak is seen at 1756 cm^{-1} that refers ester carbonyl bond of the co-polymer. Stretching vibration of C-H bond around 2945 cm^{-1} belongs to alkanes that correspond to collagen, PVP and PVA. Peaks at 1455 cm^{-1} and 1358 cm^{-1} refers to -C-H- and -CH₃ vibrations. In PVP spectrum cyclic CH₂ groups have peak at 1421 cm^{-1} and C-N stretch at 1283 cm^{-1} . PVA has a broad -OH peak at 3300 cm^{-1} corresponds to functional -OH groups of PVA. There is a peak at 1734 cm^{-1} that belongs to carbonyl group, however PVA does not have carbonyl group in its structure. The main reason is that the polymerization reaction of PVA is started with vinyl acetate and further convert to the PVA. Therefore, there is always a small amount of acetate group exist in PVA.

Removal of PVA was analyzed through FTIR spectrum as given in figure 3.7. PLLCL/PVA/0.4%Collagen and PLLCL/0.4%Collagen scaffolds after removing PVA were examined by comparing with pristine PLLCL, PVA and collagen. A small broad peak of -OH is observed at 3325 cm^{-1} and -CH peak is broadened at 1458 cm^{-1} due to PLLCL and PVA. Prior to removal of the PVA from the scaffold, only the -CH peak of the PLLCL remains and -OH peak of PVA disappears completely.

Similarly, presence and absence of PVP was also analyzed through FTIR spectrum as given in figure 3.8. In PLLCL/PVP/0.8%Collagen and PLLCL/PVP/1%Collagen scaffolds, C-N stretching of N-vinylpyrrolidone ring and -OH stretching was seen at 1292 cm^{-1} and 3430 cm^{-1} , C=O group at 1660 cm^{-1} belongs to amide. After removing PVP, all these peaks disappeared that confirms removal of PVP and only PLLCL/ Collagen remained.

Obtained results clearly indicate that PVA and PVP were successfully washed away from the scaffolds. Significant peaks cannot be obtained for collagen in PLLCL/Collagen scaffolds prior to PVA or PVP removal since collagen concentration was low and it was not in the range of FTIR.

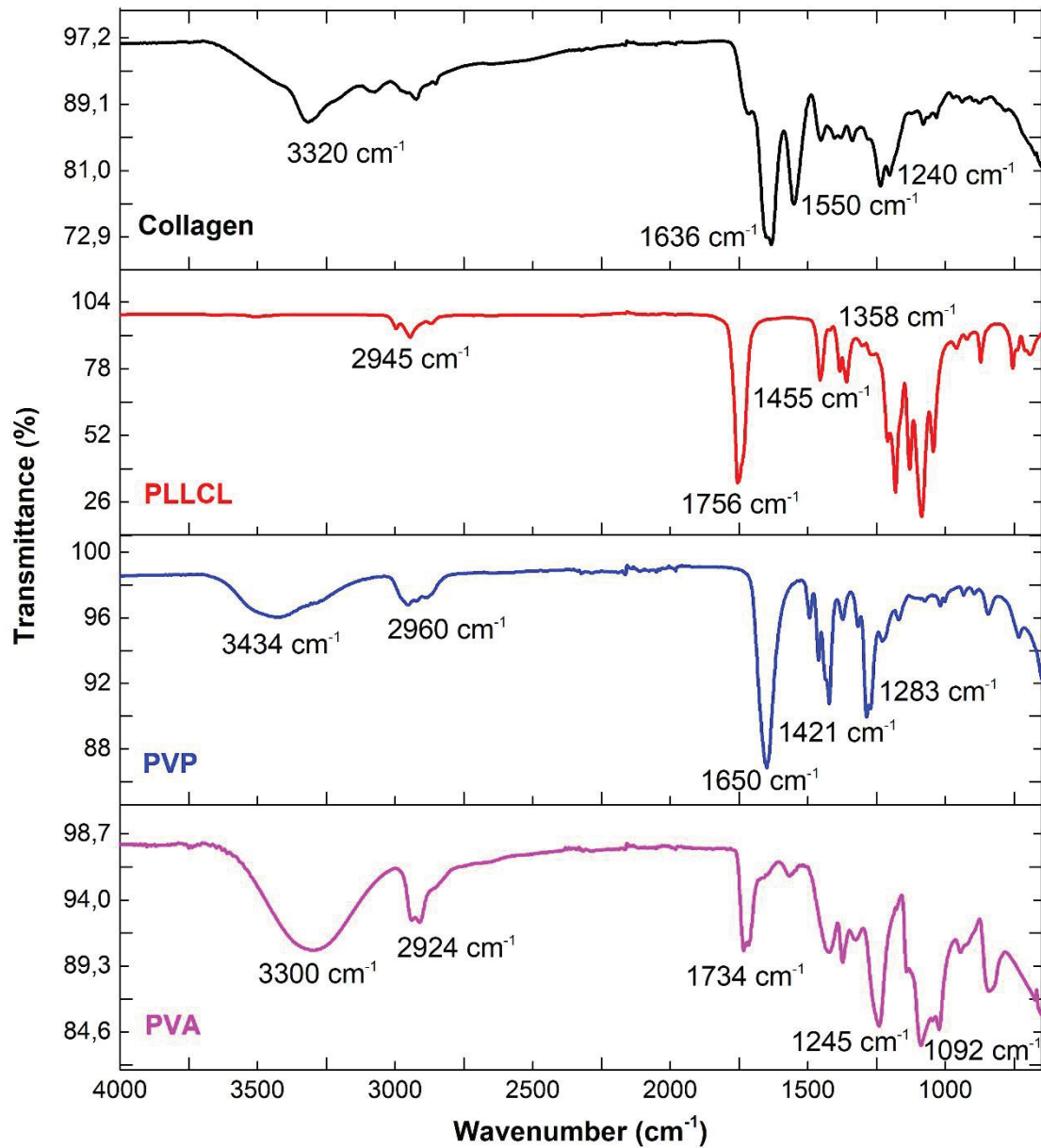


Figure 3.6. FTIR spectra of pristine Collagen, PLLCL, PVP and PVA.

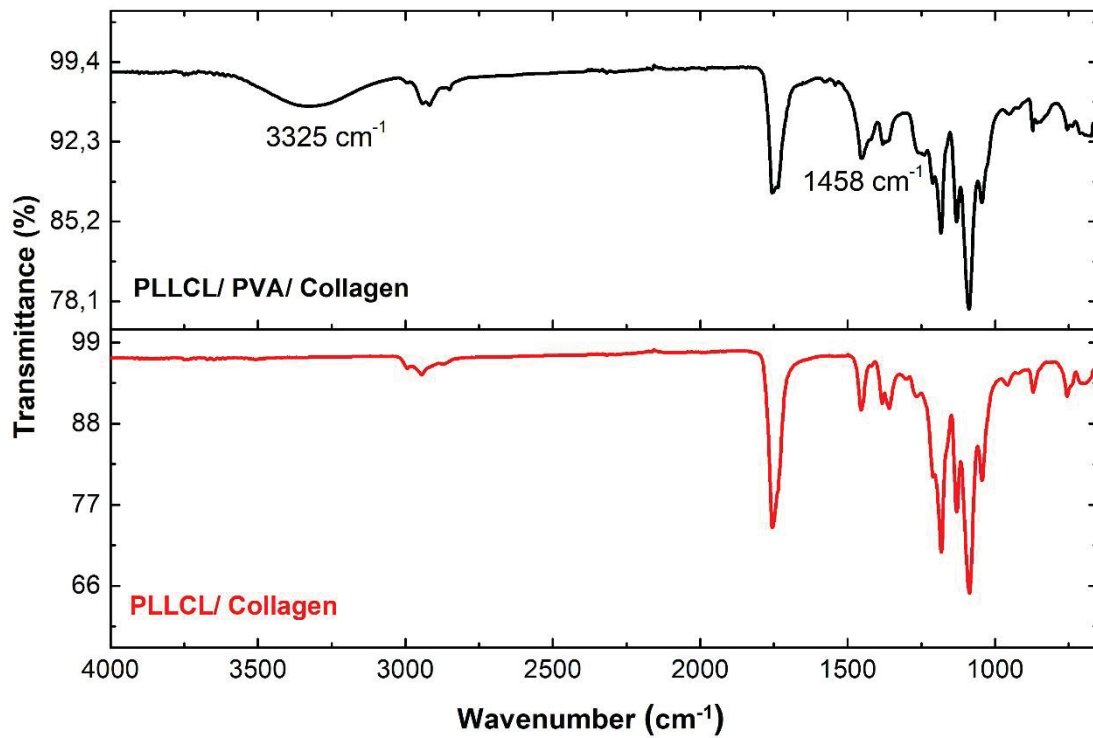


Figure 3.7. FTIR spectra of PLLCL/PVA/0.4%Collagen (black) and PLLCL/0.4%Collagen (after PVA removal) (red) scaffolds.

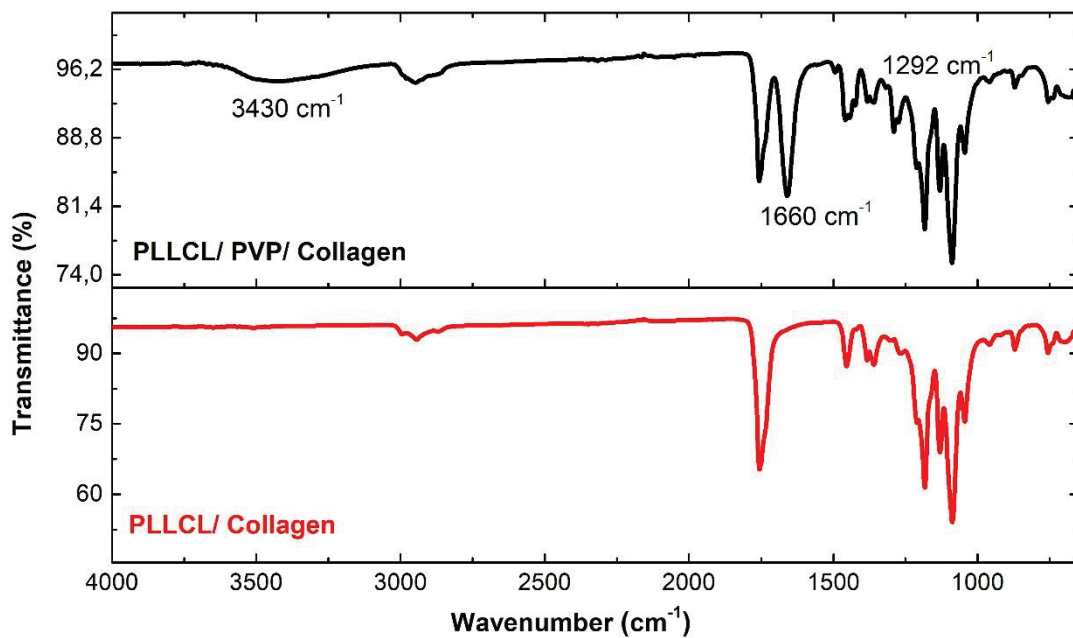


Figure 3.8. FTIR spectra of PLLCL/PVP/0.8%Collagen and PLLCL/PVP/1% Collagen (black), PLLCL/0.8%Collagen (after PVP removal) and PLLCL/1%Collagen (after PVP removal) (red) scaffolds.

3.5. Contact Angle of PLLCL/Collagen Scaffolds

Surface wettability is an important physical parameter for biomaterials that mainly affect cell adhesion, proliferation and viability.^{122, 131} Related to wettability, corresponding proteins such as; fibronectin, vitronectin, fibrinogen that guide cell attachment adhere or not on the scaffold to initiate cell substrate interaction.¹³² If the surface is too hydrophobic, protein adhesion becomes restricted and cell-substrate interaction become weak. The hydrophobic regions of proteins interact with the substrate, reducing focal adhesion and cell adhesion. In contrast, if the surface is more hydrophilic, adsorption of ECM proteins increases which also triggers the cell attachment and cell proliferation. Both circumstances should be moderate to provide good cell-cell and cell-substrate interactions.

To understand the hydrophilicity of varied concentration of collagen in PLLCL/PVA and PLLCL/PVP, static-water contact angles were measured. As represented in Table 3.1 and 3.2, PLLCL scaffold exhibits hydrophobic surface properties. When the water was dropped on PLLCL/PVA and PLLCL/PVP scaffolds, average angle was decreased due to hydrophilic property of PVA and PVP, which are water-soluble polymers. According to fiber distribution during electrospinning, water angles show differences between PLLCL/PVA/0.4%Collagen, PLLCL/0.4%Collagen (after removing PVA), PLLCL/PVP/0.8%Collagen, PLLCL/0.8%Collagen (after removing PVP), PLLCL/PVP/1%Collagen and PLLCL/1%Collagen (after removing PVP) scaffolds. In general, hydrophilic properties were observed for all above named scaffolds. When PVA and PVP removed from the scaffold, the average contact angles increased confirmed hydrophobic property, which prove the removal of PVA and PVP, and also confirms presence of collagen. Collagen is a hydrophobic protein but not as much as PLLCL. Due to the stacked form of collagen where hydrogen bond exists among amino acids (glycine, proline, hydroxyproline) and helix structure, collagen is not soluble in water.

Table 3.1. Contact angle of PLLCL and PLLCL/Collagen scaffolds with and without PVA. Results reported as mean \pm SD for three measurements.

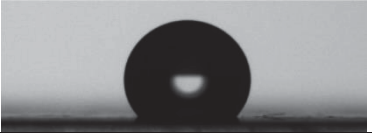





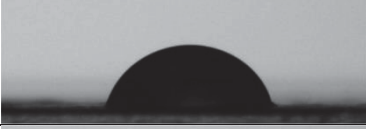
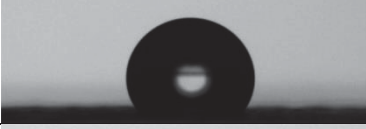


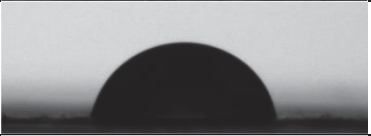

Scaffold Groups	Contact Angle (°)	Images
PLLCL	136.6° \pm 2.6	
PLLCL/ PVA	41.3° \pm 18.8	
PLLCL/PVA/0.4% Collagen	24.8° \pm 12.5	
PLLCL/0.4% Collagen	86.7° \pm 19.1	

Table 3.2. Contact angle of PLLCL and PLLCL/Collagen scaffolds with and without PVP. Contact angles reported as mean \pm SD for three measurements.

Scaffold Groups	Contact Angle (°)	Images
PLLCL	136.6° \pm 2.6	
PLLCL/ PVP	19.2° \pm 5.6	
PLLCL/ PVP / 0.4% Collagen	82.9° \pm 7.7	
PLLCL/ 0.4% Collagen	129.0° \pm 0.9	
PLLCL/ PVP / 0.8% Collagen	54.2° \pm 11.1	

(cont. on next page)

Table 3.2 (cont.).

PLLCL/ 0.8% Collagen	$95.1^\circ \pm 5.5$	
PLLCL/ PVP / 1% Collagen	$85.5^\circ \pm 7.6$	
PLLCL/ 1% Collagen	$119.0^\circ \pm 1.01$	

3.6. Protein Adsorption of PLLCL/Collagen Scaffolds

Protein adsorption can be directly related with surface properties and wettability. As mentioned previously, protein adsorption is directly related with cell-surface and cell-cell interactions, which effects the cell attachment, proliferation and differentiation.

Here, BSA solutions were analyzed as a model for protein adsorption. To determine the unknown concentration of BSA solution, calibration curve of absorbance against the known concentration of BSA was plotted (Figure 3.9).

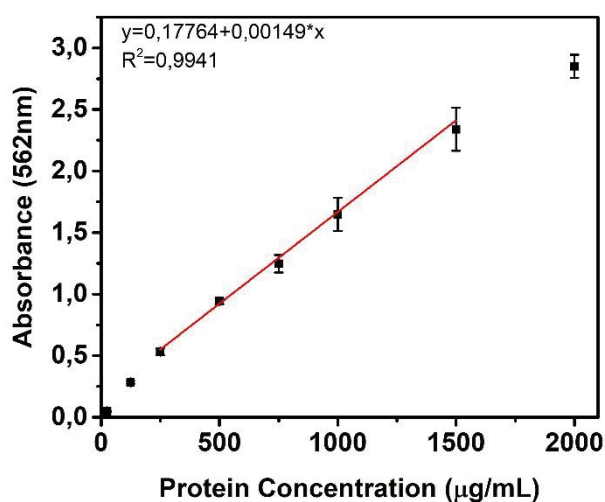


Figure 3.9. Standard calibration curve of BSA.

BSA was incubated on PLLCL, PLLCL/PVA, PLLCL/PVA/0.4%Collagen and PLLCL/PVP, PLLCL/PVP/0.8%Collagen, PLLCL/PVP/1%Collagen scaffolds. 5%w/v of Tween 80, Tween 20, TritonX-100 and SDS was used to solubilize adsorbed BSA on PLLCL scaffolds (Figure 3.10). There was a background interference problem with the BCA kit when Tween 80 was utilized.¹³³⁻¹³⁴ Among the other detergents SDS provided the most correlated results, so SDS was preferred for further characterization steps.

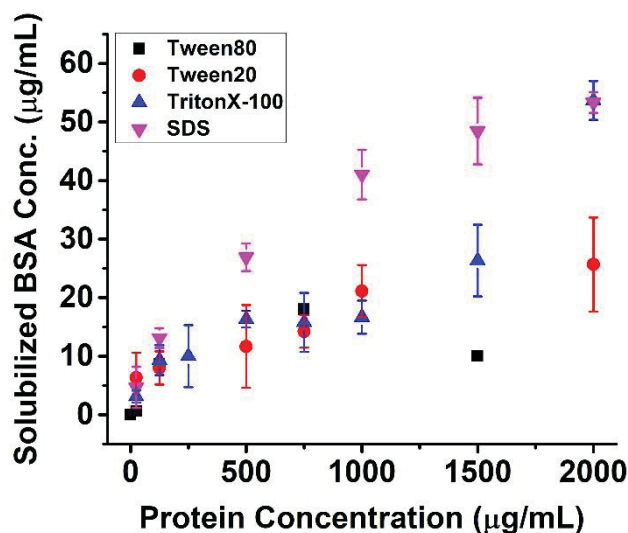


Figure 3.10. Solubilizing adsorbed BSA on PLLCL scaffold with Tween80, Tween20, TritonX-100 and SDS.

Amount of adsorbed proteins on scaffolds shows a steady increase during 2h incubation (Figure 3.11). After rinsing with 1X PBS, weakly attached BSA on the surface was removed and only tightly bounded BSA molecules remained. For this reason, the exact amount of adsorbed protein on the scaffold was determined through solubilization by SDS.

Figure 3.12 gives the solubilized BSA on scaffolds. According to these results, PLLCL scaffold saturates at 43 µg/mL, PLLCL/PVA 33 µg/mL, PLLCL/PVA/0.4%Collagen 23 µg/mL, PLLCL/PVP 30 µg/mL, PLLCL/PVP/0.8%Collagen 14 µg/mL, PLLCL/PVP/1%Collagen scaffold 9 µg/mL.

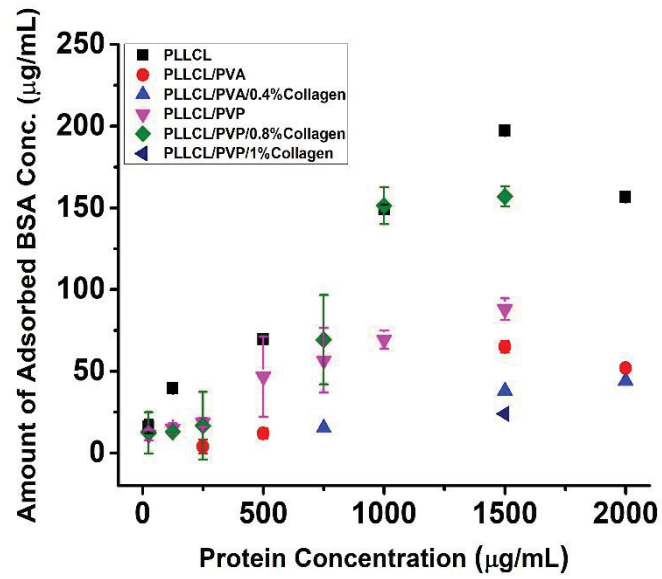


Figure 3.11. Weakly adsorbed BSA on scaffolds.

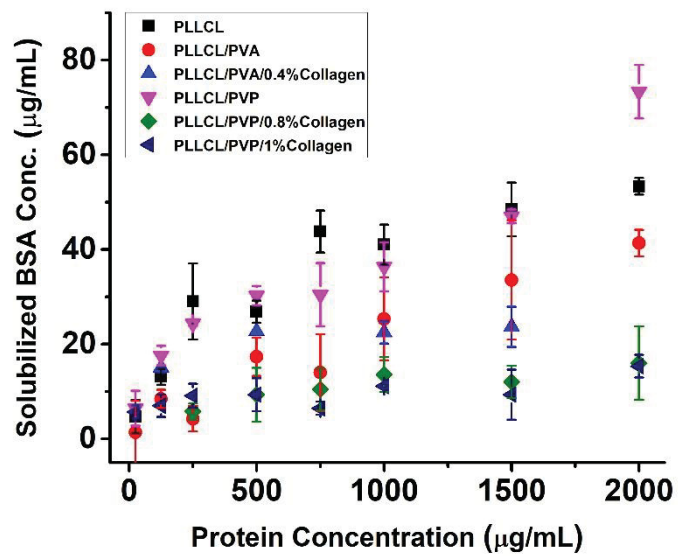


Figure 3.12. Solubilized BSA on scaffolds.

3.7. Mechanical Characterization with Tensile Test

Mechanical characterization of PLLCL, PLLCL/PVP, PLLCL/PVP/0.8%Collagen, PLLCL/0.8%Collagen (after PVP removal), PLLCL/PVP/1%Collagen and PLLCL/1%Collagen (after PVP removal) scaffolds were

determined by tensile test which performed by using TA. XT Texture Analyzer (Stable Micro Systems).

By stretching random coil chains are forced to be uncoiled and the extent of secondary interactions intensified among polymer chains. The electrospinning process lead the chains close-packing due to orientation along the fibers therefore mechanical properties materials are expected to be improved as compare to bulk polymers. As tension applied to the fiber mats along the direction of the fibers, an anomalous strain response observed due to collective response of fibers. The fibers which are shorter than medium length or fibers perpendicular to the stress direction were contributing by lowering the mechanical strength. Mechanical properties of scaffolds demonstrated at table 3.3; PLLCL scaffold exhibit larger elongation strain than PLLCL/ PVP whereas lower tensile modulus than PLLCL/ PVP scaffold assuring that PVP was reinforced PLLCL scaffold but reduces its strength of elongation.

Table 3.3. Tensile tests result of scaffolds. Results reported as mean \pm SD for four measurements.

Scaffold Groups	Tensile Modulus, MPa	Ultimate Tensile Strength, MPa	Elongation at Break, %
PLLCL	1.15 \pm 0.02	2.90 \pm 0.34	262 \pm 15.9
PLLCL/ PVP	6.32 \pm 2.6	1.13 \pm 0.01	25 \pm 5.8
PLLCL/ PVP/ 0.8%Collagen	0.648 \pm 0.04	1.16 \pm 0.33	195 \pm 18.6
PLLCL/ 0.8%Collagen	1.03 \pm 1.0	1.59 \pm 0.28	161 \pm 27.3
PLLCL/ PVP/ 1%Collagen	1.012 \pm 0.06	1.84 \pm 0.27	202 \pm 12.1
PLLCL/ 1% Collagen	1.84 \pm 0.16	4.27 \pm 0.16	245 \pm 7.2

Owing to low molecular weight of PVP, directly weakened mechanical abilities of the materials. While ultimate tensile strength was compared, PVP removed scaffolds showed higher strength than PVP containing scaffold. The, PLLCL/PVP/1%Collagen and PLLCL/1%Collagen (after PVP removal) exhibit the highest tensile strength as expected. By the removal of PVP, the scaffold shows better elongation and increase in the tensile modulus due to semi-oriented conformation of fibers by hydrogen bonding of collagen (Figure 3.13). Additionally, strength directly increases by the removal of PVP from the scaffold that assures shorter chain length polymer weakens the tensile strength. Overall, tensile test results indicate PVP reduces mechanical stiffness

(strength), on the other hand collagen fibrillar structure and hydrogen bonding of the structure provide to increase the strength of the scaffold.

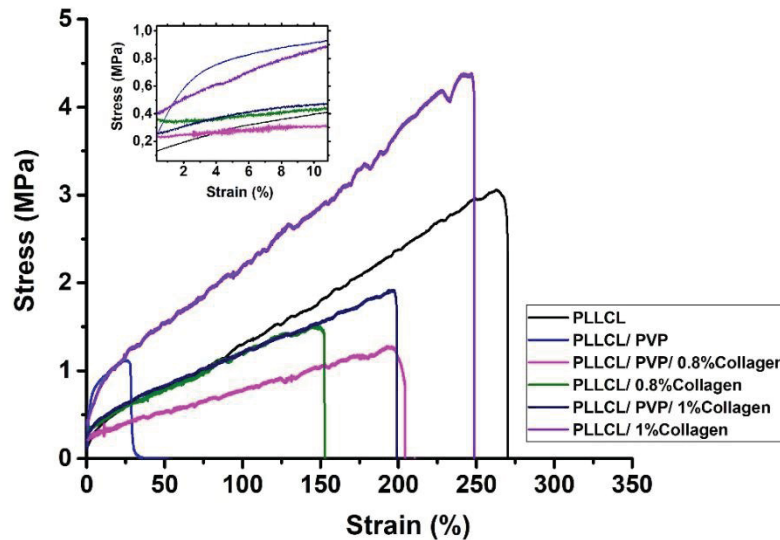


Figure 3.13. Stress-strain curve of PLLCL, PLLCL/ PVP, PLLCL/PVP/0.8%Collagen, PLLCL/%0.8Collagen (after PVP removal), PLLCL/PVP/1%Collagen and PLLCL/1%Collagen (after PVP removal).

3.8. Hydrolytic and Enzymatic Biodegradation of PLLCL Scaffolds

PLLCL (70:30) is a co-polymer where semi-crystalline poly (L-lactide) (PLLA) and poly (ϵ -caprolactone) (PCL) linked by ester bond. Hydrolytic degradation takes place via scission of ester linkage in the backbone of the PLLCL. As a degradation product, lactic acid and caproic acid is formed that can be metabolized easily in a body. There are many parameters that affect hydrolytic degradation such as molecular weight, temperature, hydrophilicity/ hydrophobicity, intensity of ester groups and degradation media. Crystallinity is an important factor since during hydrolysis, degradation media initially penetrate amorphous region of the polymer. PCL is more packed instead of PLA, so water penetration takes time and leads to degradation in slower rate.¹³⁵⁻¹³⁸

In this study, temperature kept constant at 37°C as same as human body. During the hydrolytic degradation of PLLCL in 20-week analysis, PLLCL scaffolds started to lose mass at the 13th week and weight loss was 12.1% at the end of 20 weeks (Figure 3.14a). In the first 13 weeks, there was no much change in weight. Based on SEM analysis of degraded PLLCL scaffolds (Figure 3.15), hydrolytic degradation was

observed where polymer fibers started to be cleaved after 13th week up to 20th-week. Also, porosity of the scaffold increased from 9th week ($17.2\% \pm 1.74$) to 20th week ($34.4\% \pm 2.99$) (Figure 3.14b).

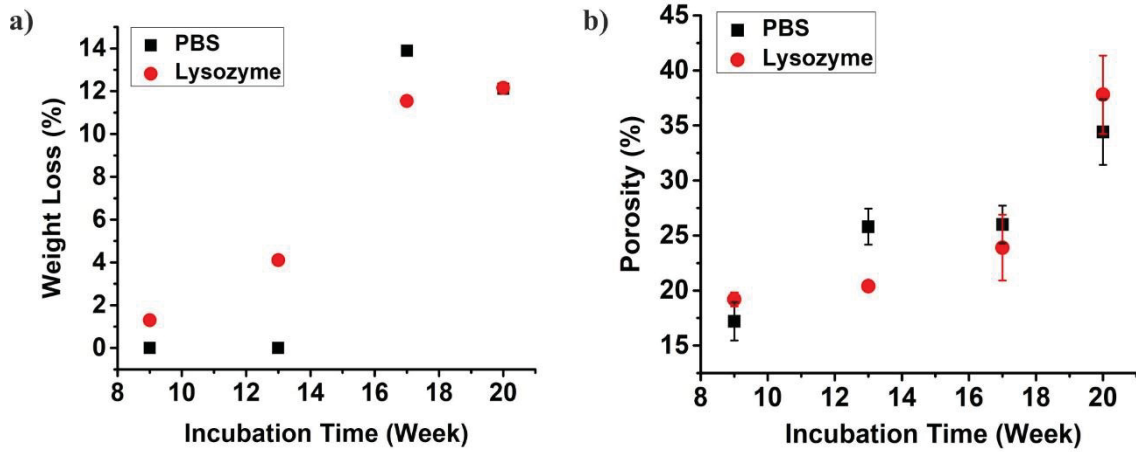


Figure 3.14. *In vitro* biodegradation analysis of PLLCL in 20week incubation period, a) weight loss and b) porosity against weeks.

Enzymatic degradation was applied on PLLCL. Apparently, degradation rate of lysozyme on PLLCL was higher than hydrolytic degradation. The weight lost because of enzymatic degradation was found to be higher compared to the hydrolytically degrading samples (Figure 3.14a). The weight loss in 9th week was 1.3%, and in 13th week it was around 4.1%. There was no significant change in the 17th and 20th weeks, 11.5% and 12.1% respectively. At 20th week both hydrolytic and enzymatic degraded PLLCL has the same weight loss 12.1%. Further, the porosity increases gradually rather than hydrolytically degraded PLLCL which reached to $37.8\% \pm 3.56$ at 20th week (Figure 3.14b). When the morphological structures of the fibers are examined (Figure 3.16), pores were formed even on the surface of the fibers. It shows that surface erosion type degradation occurs when the lysozyme is utilized for the degradation process of PLLCL. The formation of porosity can be attributed to the fibrous deformation over time. These results indicate that erosion was started with chain cleavage, which is related with mass loss.

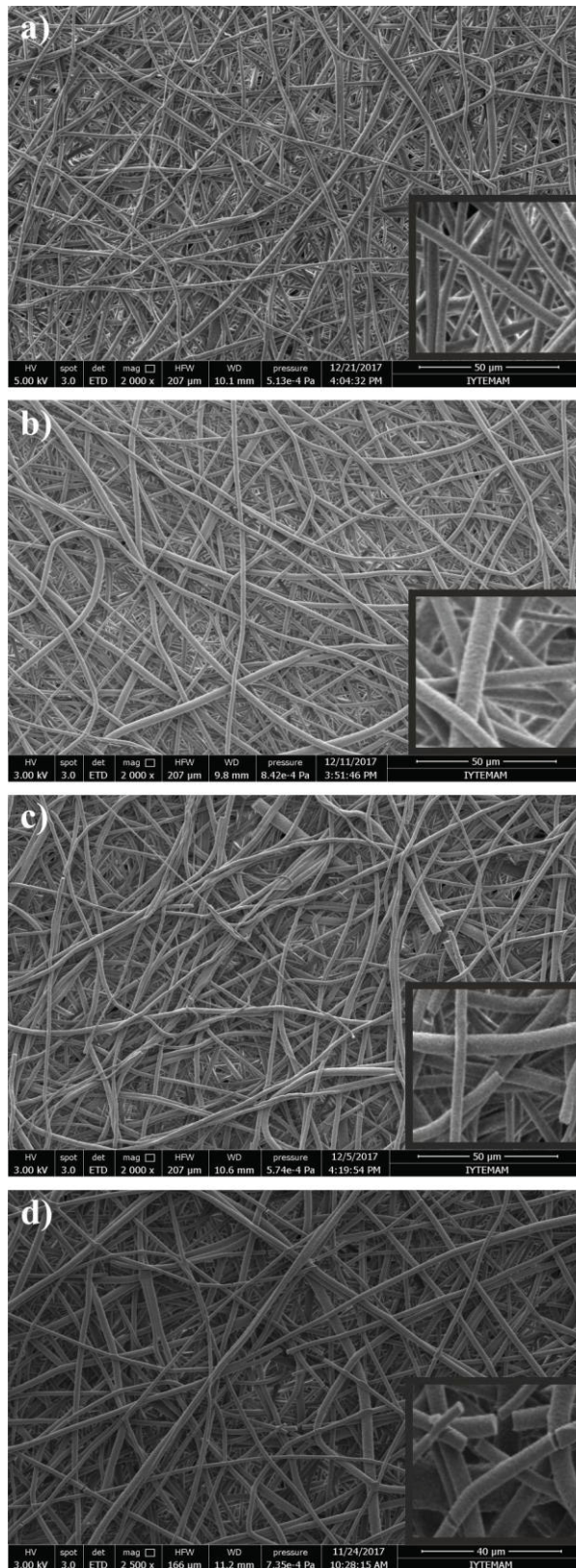


Figure 3.15. SEM micrographs of hydrolytic degradation of PLLCL a) 9th week, b) 13th week, c) 17th week and d) 20th week.

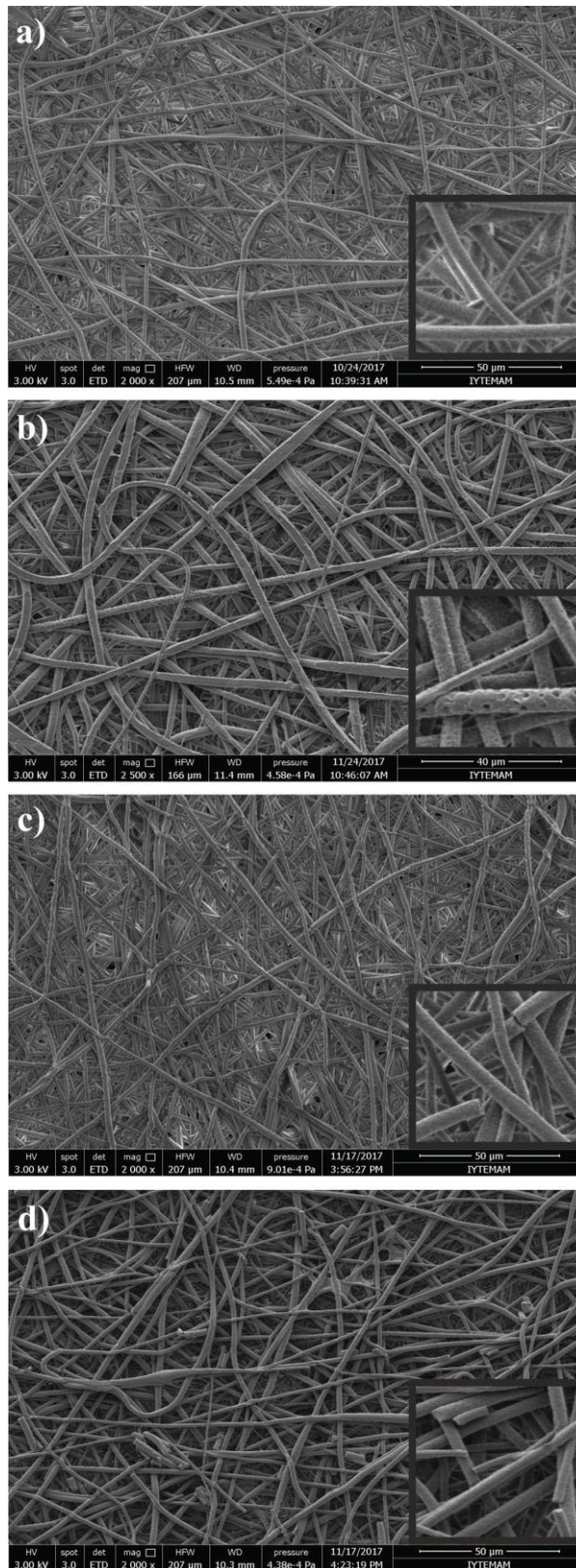


Figure 3.16. SEM micrograph of enzymatic degradation of PLLCL a) 9th week, b) 13th week, c) 17th week and d) 20th week.

3.9. *In vitro* 3D Cell Culture Studies

3.9.1. *In vitro* Proliferation Assay on PLLCL/Collagen Scaffolds

Proliferation behavior of NIH3T3 mouse fibroblast were examined for 1, 3, 5 and 7day incubation periods. Proliferation of NIH3T3 cells on PLLCL, PLLCL/ PVA, PLLCL/PVA/0.4%Collagen, PLLCL/0.4%Collagen (after removing PVA) and PLLCL/ PVP, PLLCL/PVP/0.4%Collagen, PLLCL/0.4%Collagen (after removing PVP) 3D scaffolds was analyzed with MTT assay against 2D control groups. In figure 3.17, PLLCL/PVA, PLLCL/PVA/0.4%Collagen and PLLCL/0.4%Collagen (after removing PVA) scaffolds did not show a significant effect on proliferation compared to PLLCL, PLLCL/PVP/0.4%Collagen and PLLCL/0.4%Collagen (after removing PVP) scaffolds that shows high proliferation from 1st day to 7th day.

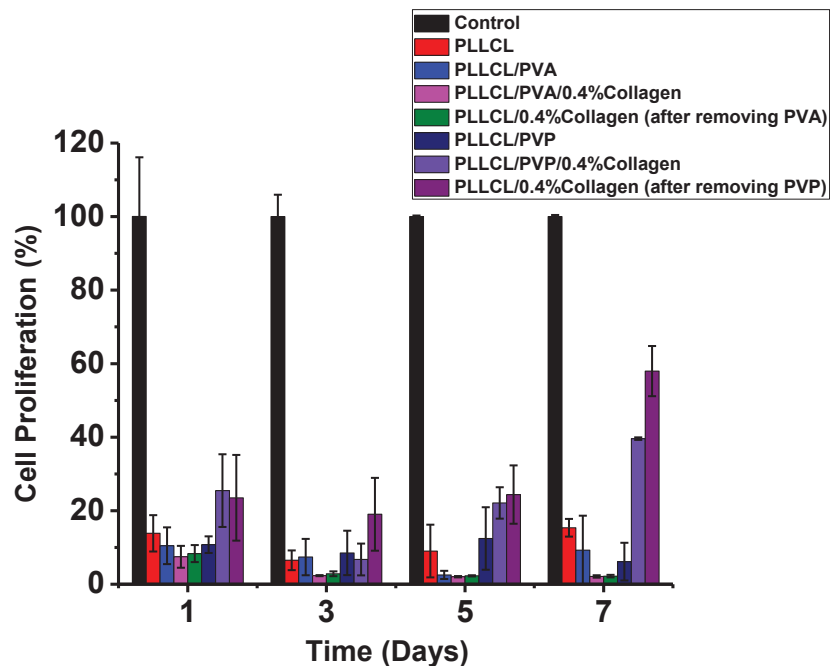


Figure 3.17. MTT assay results of NIH3T3 cell proliferation on PLLCL, PLLCL/ PVA, PLLCL/PVA/0.4%Collagen, PLLCL/0.4%Collagen (after removing PVA), PLLCL/PVP, PLLCL/PVP/0.4%Collagen, PLLCL/0.4%Collagen (after removing PVP) scaffolds in 1, 3, 5 and 7 days cell culture periods.

Even at the repeating experiments, PLLCL/PVA, PLLCL/PVA/0.4%Collagen and PLLCL 0.4% Collagen (after removing PVA) scaffolds shows low proliferation until 3 days. In the rest of the days, cells attachment is favored on PLLCL/PVP, PLLCL/PVP/0.4%Collagen and PLLCL/0.4%Collagen (after removing PVP) scaffolds. Since collagen is the key point that provide cell attachment cell proliferation on PLLCL, which was the positive 3D control, was compared to PLLCL/PVA/0.4%Collagen and PLLCL/0.4%Collagen (after removing PVA) scaffolds. While PVP was washed away and removed from the scaffold, proliferation of cells increased more than PLLCL itself. Since proliferation results of PVP-based polymer scaffolds provided better results compared to PVA-based ones further experiments conducted with PVP-based polymer scaffolds.

During MTT analysis background problem occurred based on optical readings since non-transparent polymer scaffolds were used. At the same time polymer scaffolds were dissolved in DMSO while performing MTT assay. Therefore, same experiments were performed with alamar blue assay on PLLCL, PLLCL/PVP, PLLCL/PVP/0.8%Collagen, PLLCL/0.8%Collagen (after removing PVP) and PLLCL/PVP1%Collagen, PLLCL/1%Collagen (after removing PVP) scaffolds for 7day incubation period. Cell attachment and adaptation of NIH3T3 mouse fibroblast cells on PLLCL/PVP scaffold takes around 5days, however cells on PLLCL/PVP/0.8%Collagen, PLLCL/0.8%Collagen (after removing PVP) and PLLCL/PVP/1%Collagen, PLLCL/1%Collagen (after removing PVP) scaffolds started to proliferate after first day of incubation and the cell number increased up to 7days. In the first 3 days, PLLCL scaffold showed higher proliferation than PLLCL/PVP, PLLCL/PVP/0.8%Collagen, PLLCL/0.8%Collagen (after removing PVP) and PLLCL/PVP/1%Collagen, PLLCL/1%Collagen (after removing PVP) scaffolds. Both 0.8% Collagen and 1% Collagen containing scaffolds with and without PVP had not a significant change. However, as specified in figure 3.18, collagen contained scaffolds ensures initial attachment of cells and showed moderate increase instead of PLLCL and PLLCL/ PVP scaffolds.

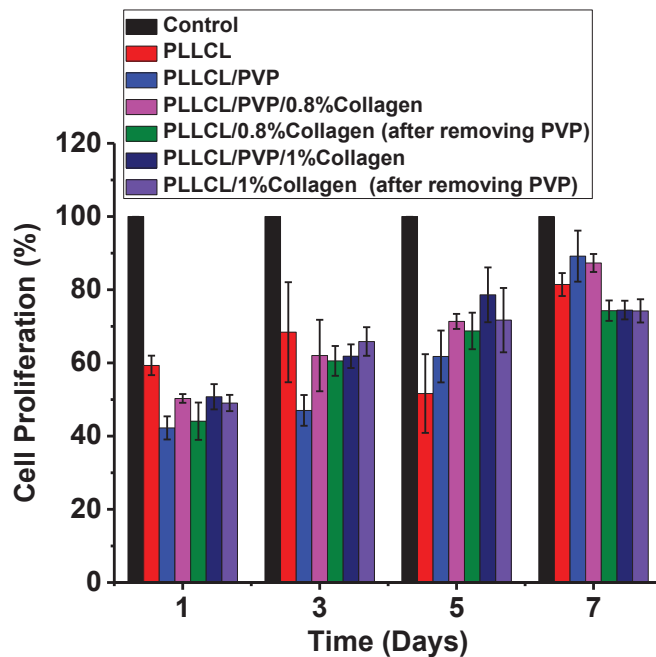


Figure 3.18. Alamar blue assay results of NIH3T3 cell proliferation on PLLCL, PLLCL/PVP, PLLCL/PVP/0.8%Collagen, PLLCL/0.8% Collagen (after removing PVP), PLLCL/PVP/1%Collagen and PLLCL/1%Collagen (after removing PVP) scaffolds for 1, 3, 5 and 7day cell culture period.

3.9.2. Cell Viability Assay on PLLCL/Collagen Scaffolds

Cell viability of NIH3T3 mouse fibroblast cells on PLLCL, PLLCL/PVA, PLLCL/PVA/0.4%Collagen, PLLCL/0.4%Collagen (after removing PVA) and PLLCL/PVP, PLLCL/PVP/0.4%Collagen, PLLCL/0.4%Collagen (after removing PVP) 3D scaffolds were examined through live/dead assay shown in figure 3.19. Control groups were grown in 2D similar to MTT and alamar blue assays. NIH3T3 cells adhere on PLLCL scaffolds, started to proliferate at 3rd day, cell number increased up to 5th day but cell deaths (red stained cells) started at 7th day. Especially PLLCL/PVA scaffold had small agglomerations of cells and it was observed that cells tend to proliferate only around agglomerated area. At 5th day, cell death increased compared to viable cells, which can be the effect of acidic groups of PVA. Even at PLLCL/PVA/0.4%Collagen and PVA washed PLLCL/0.4%Collagen scaffolds, agglomerated cells were observed due to trace amount of remaining PVA in the environment. At day 7, rate of the cell death was increased around cell agglomerations. Compared to PVA, PVP-based scaffolds provided higher cell viability. Moreover, cell proliferation increased

proportionally incubation time and cells spread over the scaffold particularly in PLLCL/PVP/0.4%Collagen and PLLCL/0.4% collagen (after removing PVP) scaffolds.

When the collagen concentration was increased in the scaffold cell attachment, proliferation and viability also increased. Cell viability of NIH 3T3 mouse fibroblast cells was performed for PLLCL, PLLCL/PVP/0.8%Collagen, PLLCL/0.8%Collagen (after removing PVP), PLLCL/PVP/1%Collagen and PLLCL/1%Collagen (after removing PVP) scaffolds (Figure 3.20). PLLCL scaffolds had higher viability than PLLCL/PVP. The toxic effect of PVP could be seen at PLLCL/PVP/0.8%Collagen and PLLCL/PVP/1%Collagen scaffold that had lower viability and higher cell death than PLLCL/0.8%Collagen (after removing PVP) and PLLCL/1%Collagen (after removing PVP) scaffolds. Additionally, by increasing collagen concentration from 0.4% to 1%, proliferation behavior and viability of NIH3T3 cells increased. As expected collagen containing scaffolds provide suitable microenvironment and mimic the ECM for homogeneous cell attachments, and also prevent agglomeration of the cells on 3D scaffolds.

Cell proliferation behavior and viability was also analyzed for long-term culturing conditions by using PLLCL, PLLCL/PVP, PLLCL/PVP/1%Collagen and PLLCL/1%Collagen (after removing PVP) scaffolds (Figure 3.21) for 1, 7, 11 and 15day incubation period. 2D control group was reached to maximum confluency at 11th day, and cells over proliferate at 13th and 15th day. Due to increased cell number, cells started detaching from the surface and floated in the medium. Lowest viability was observed for PLLCL/PVP scaffold compared to others. On the other hand, PLLCL/PVP/1%Collagen and PLLCL/1%Collagen (after removing PVP) scaffolds provided the highest viability and confluency.

All these results showed that collagen is the key point for cells attachment, proliferation and viability. PLLCL itself is a biocompatible material and as showed good biocompatibility on cells. However, addition of collagen improved the biocompatibility of the scaffolds. At the same time, using PVP as a co-spinning or sacrificing agent for collagen spinning was successfully achieved, and proved that fabrication scaffolds can be easily utilized for 3D cell culturing studies.

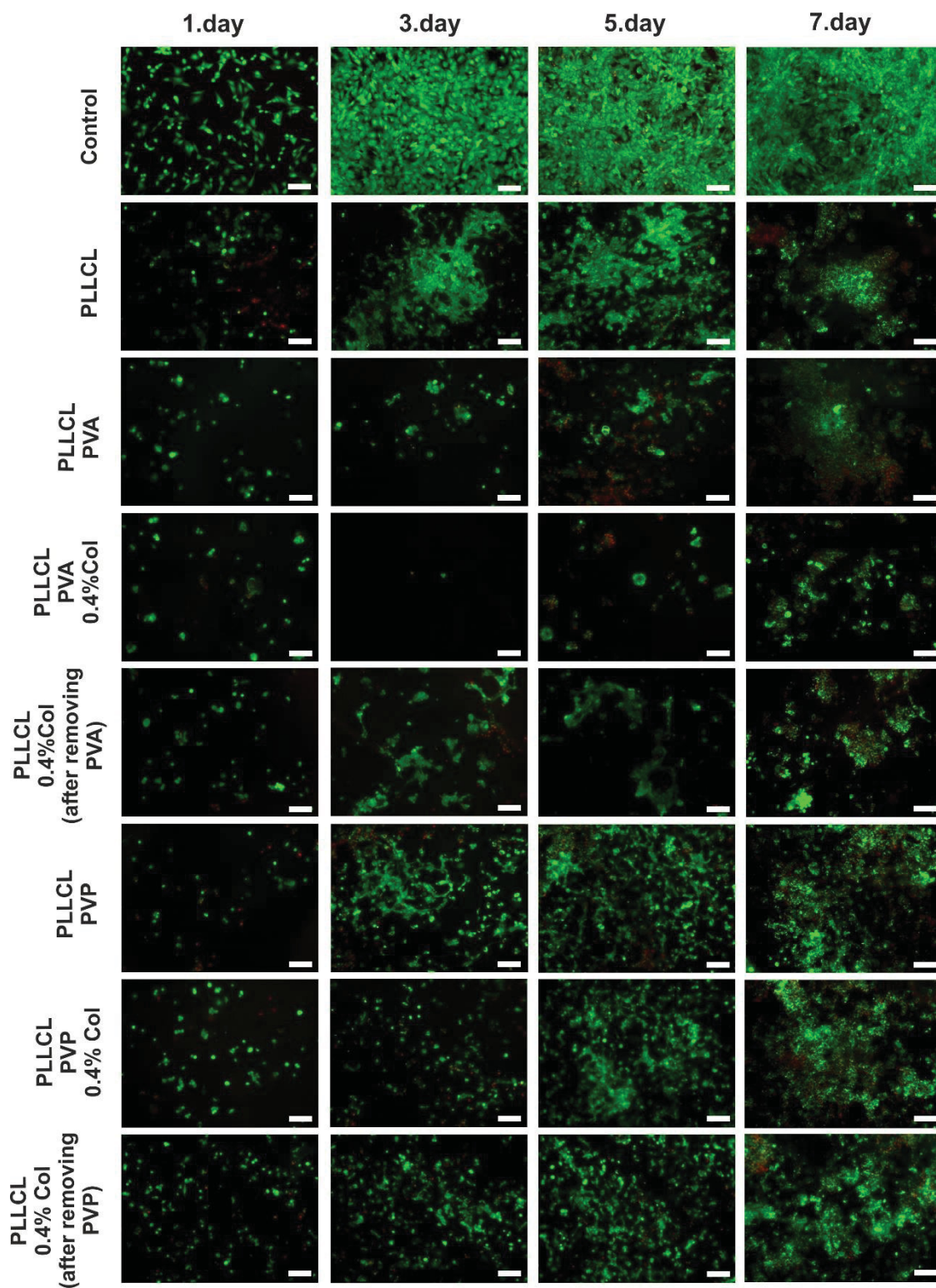


Figure 3.19. Fluorescence microscope images of live/ dead assay on PLLCL, PLLCL/PVA, PLLCL/PVA/0.4%Collagen, PLLCL/0.4%Collagen (after removing PVA) and PLLCL/PVP, PLLCL/PVP/0.4%Collagen, PLLCL/0.4%Collagen (after removing PVP) scaffolds for 1, 3, 5 and 7day cell culture periods (scale bar 100 μ m). Green represents live cells, red represents dead cells.

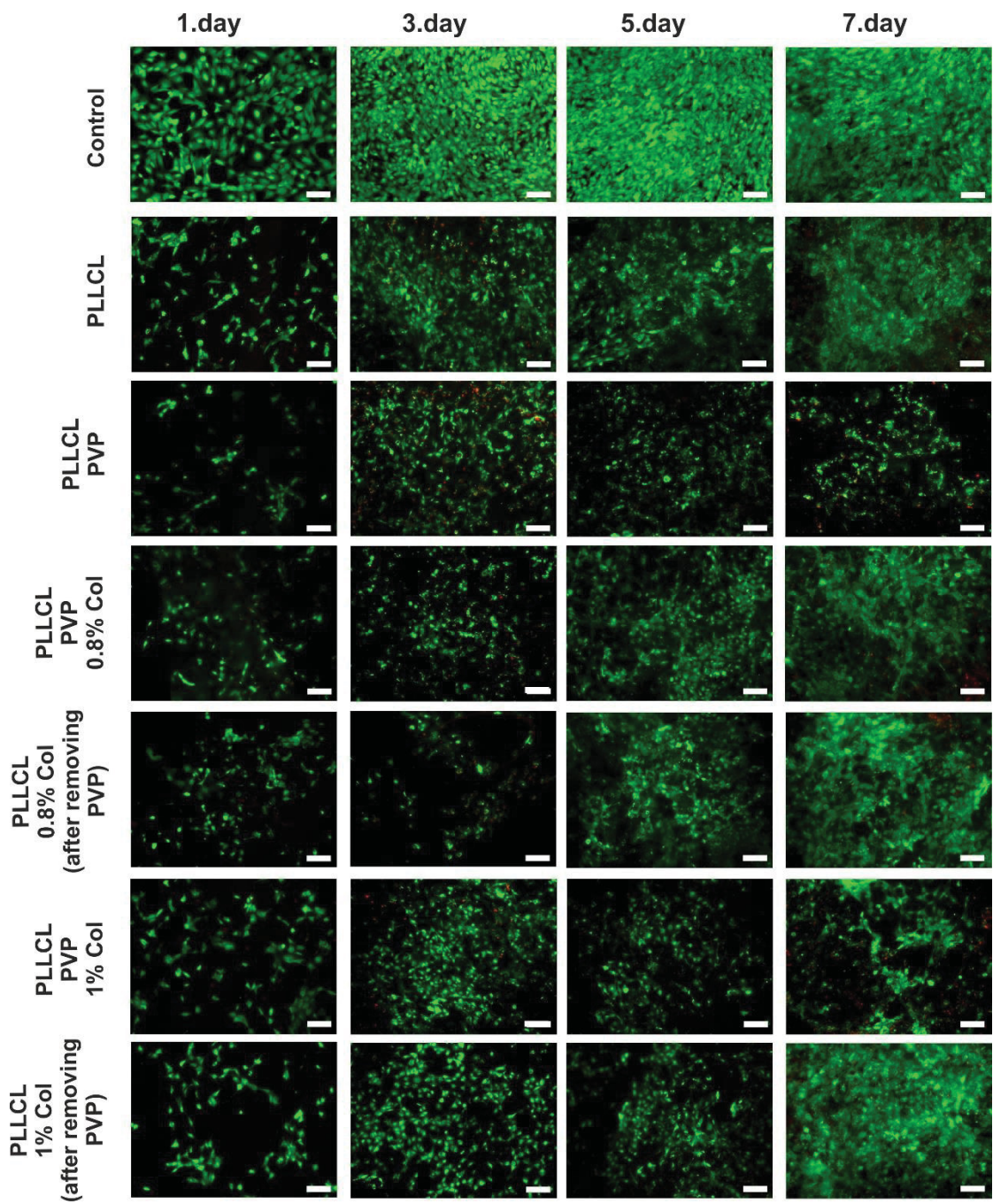


Figure 3.20. Fluorescence microscope images of live/ dead assay on PLLCL, PLLCL/PVP, PLLCL/PVP/0.8%Collagen, PLLCL/0.8%Collagen (after removing PVP) and PLLCL/PVP/ 1%Collagen, PLLCL/1%Collagen (after removing PVP) scaffolds for 1, 3, 5 and 7day cell culture periods (scale bar 100 μ m). Green represent live cells, red represents dead cells.

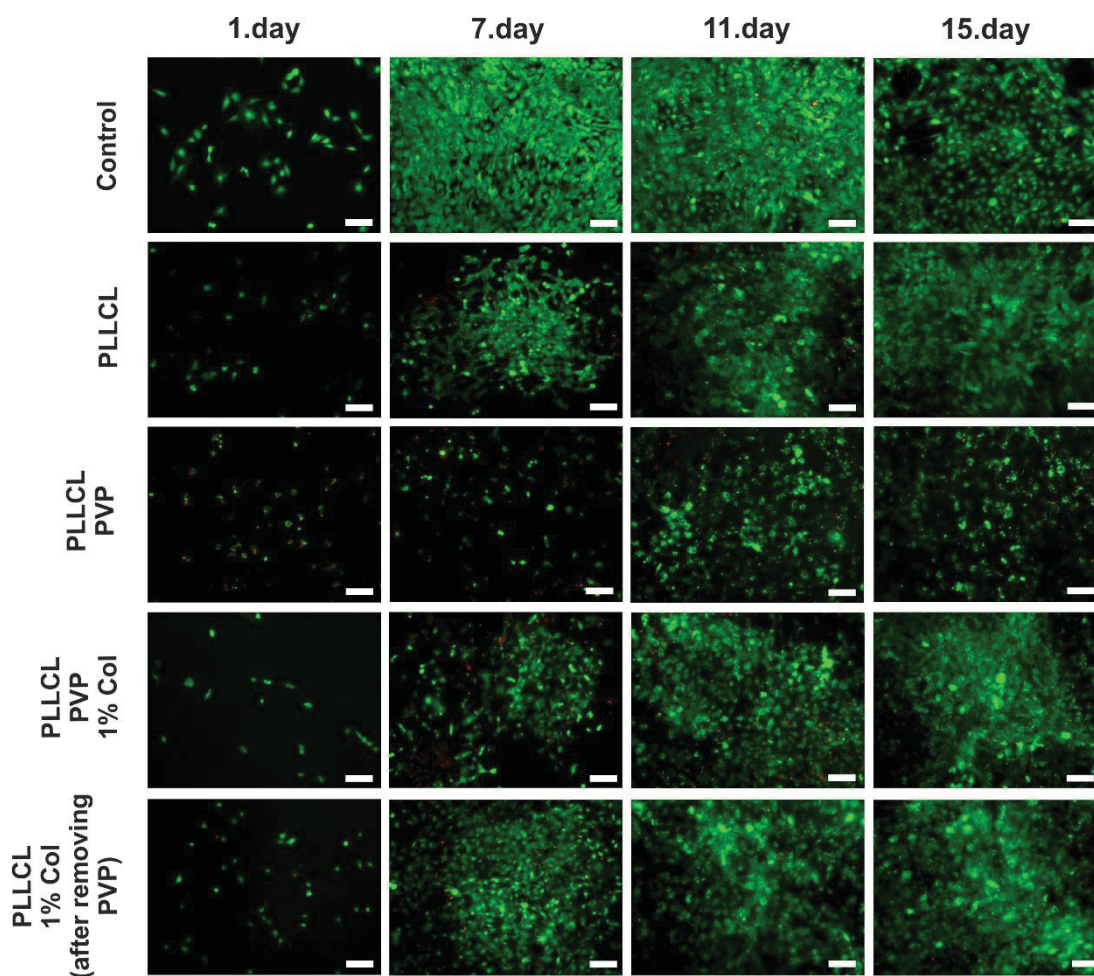


Figure 3.21. Fluorescence microscope images of live/ dead assay on PLLCL, PLLCL/PVP, PLLCL/PVP/1%Collagen and PLLCL/1%Collagen (after removing PVP) scaffolds for 1, 7, 11 and 15day cell culture periods (scale bar: 100 μ m). Green represent live cells, red represents dead cells.

3.9.3. SEM Cell Analysis of Cell Attachment on PLLCL/Collagen Scaffolds

The cell attachment and proliferation behavior of NIH3T3 mouse fibroblast cells on PLLCL/Collagen scaffolds were examined by SEM at 1, 3, 5 and 7days cell culture periods (Figure 3.22). Cell attachment and morphological changes of NIH 3T3 cells were clearly observed in 1 day. After 3 days, NIH 3T3 cells completely spread and stretched over polymer fibers. Parallel to the incubation time, cells started to cover scaffolds and the increasing cell number indicates that 3D scaffold favors the cell proliferation. These results demonstrated that PLLCL/Collagen scaffold has good

biocompatibility for 3D cell culturing studies and provides suitable microenvironment, which behaves like ECM for NIH 3T3 cells.

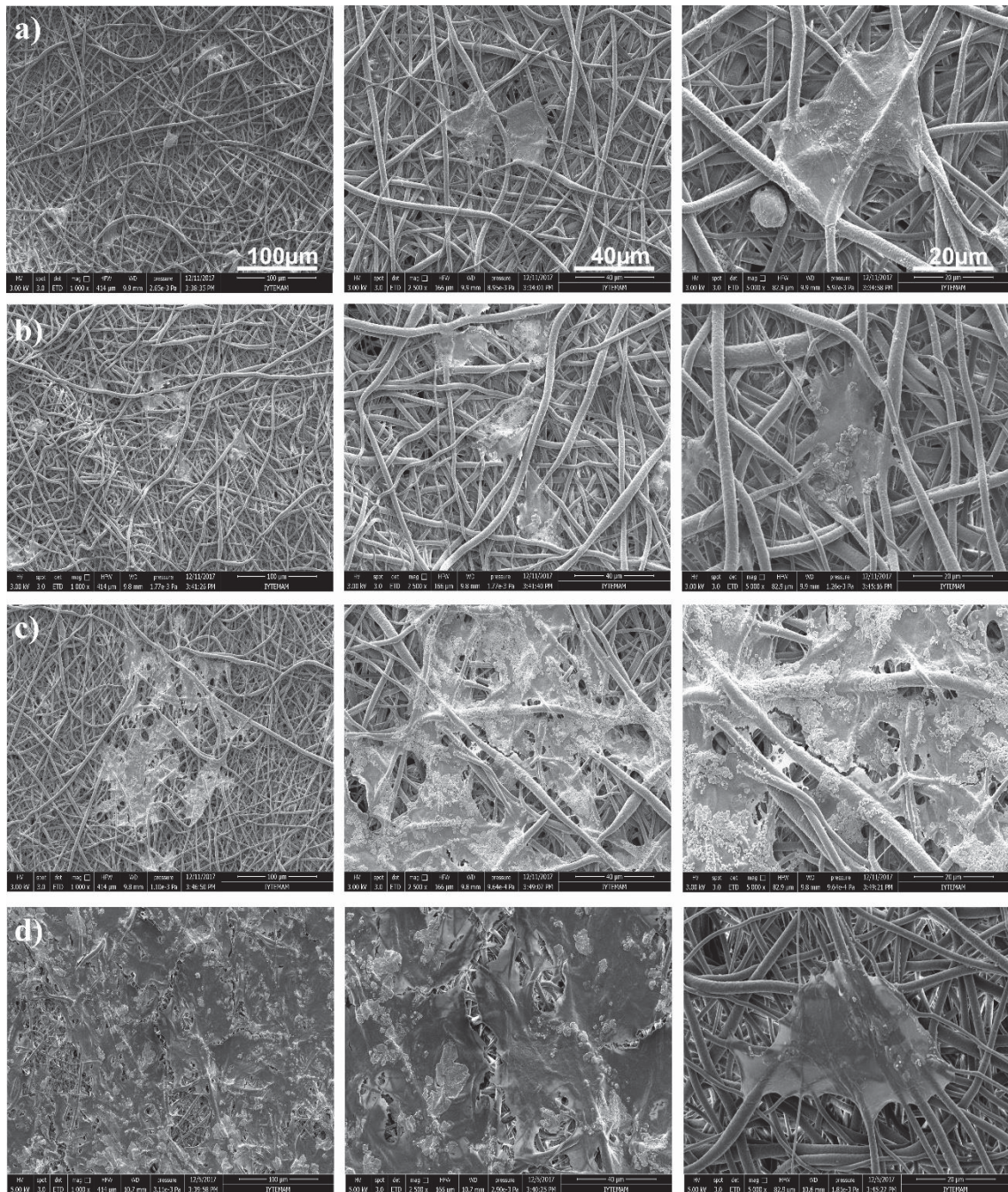


Figure 3.22. Cell attachment and proliferation behavior of NIH 3T3 cells on PLLCL/0.4%Collagen (after PVP removal) scaffolds in a) 1st day, b) 3rd day, c) 5th day and d) 7th day cell culture periods.



Figure 3.23. SEM micrograph of NIH 3T3 cell attached on PLLCL/0.4%Collagen fibers.

Under biological environment cell attachment occurs through cell-ECM interaction. As shown in figure 3.23, attachment of NIH 3T3 cells on electrospun PLLCL/Collagen fiber surface and formation of small cellular extensions, which favors cell adhesion, was also observed via SEM analysis.

CHAPTER 4

CONCLUSION

In tissue engineering applications synthetic and natural materials are mostly utilized as cell culture scaffolds to support by physical and biochemical properties. Synthetic materials provide mechanical stability, strength, biodegradability, on the other hand natural materials ensures biocompatibility, and favors cell adhesion, proliferation and migration. Therefore, composite materials are becoming more applicable for tissue engineering applications by complementing the missing properties of both materials. After selecting proper biomaterials, the fabrication technique is also an important parameter. Because each biofabrication technique has its own advantages and drawbacks. In this study, electrospinning technique is preferred since it is an advanced fabrication technology and nanofiber structures can be easily formed. Particularly, this methodology is useful while mimicking the fibrillar structure of collagen that widely found in natural ECM.

Processing collagen is not easy due to its non-soluble characteristics. In most studies, collagen is solubilized and processed with HFIP solvent, which is a very toxic chemical and not preferable to use for biological applications. Therefore, low concentration of acetic acid solution was used to dissolve the collagen and mixed with PLLCL. Because of the polarity difference of solvents collagen precipitated. To overcome this problem co-electrospinning agent; PVA and PVP that are water soluble, was used. Polarities of both solvents (water and acetic acid) are close, so when the collagen and PVA or PVP solution is mixed homogeneous solution was obtained without precipitation. Here, it was demonstrated that PLLCL and PVA/Collagen, PLLCL and PVP/Collagen scaffolds were fabricated successfully through co-electrospinning technique. Later co-spinning agents, namely sacrificing agents were easily removed from scaffolds by solubilizing in water. According to cell experiments, PVA including or removed scaffolds exhibited lower proliferation and viability, so the PVP-based scaffolds were utilized for further studies.

All in all, a new methodology has been developed to electrospun the collagen by avoiding heavy chemicals. Characterization and cell experiments support the achievement of this method. Presence and absence of PVP, existence of collagen on

PLLCL scaffolds were shown by FTIR and collagen immunostaining. Mechanical strength of collagen including scaffolds had higher strength due to fibrillar structure of PLLCL and collagen that reinforce each other. In 3D cell culture experiments, collagen including scaffolds had higher viability because collagen is the key component of natural ECM that provides cell adhesion, migration and differentiation. Also, SEM images were supporting the spreading and differentiation of NIH 3T3 cells on PLLCL/Collagen 3D scaffolds.

REFERENCES

1. Boateng, J.; Catanzano, O., Advanced Therapeutic Dressings for Effective Wound Healing--A Review. *J Pharm Sci* **2015**, *104* (11), 3653-80.
2. Badylak, S. F.; Taylor, D.; Uygun, K., Whole-organ tissue engineering: decellularization and recellularization of three-dimensional matrix scaffolds. *Annu Rev Biomed Eng* **2011**, *13*, 27-53.
3. Vacanti, R. L. a. J. P., Tissue Engineering. *Science* **1993**, *260*, 920-926.
4. Babita Mahanta, R. N., An Overview of Various Biomimetic Scaffolds: Challenges and Applications in Tissue Engineering. *Journal of Tissue Science & Engineering* **2014**, *05* (02).
5. Wang, X.; Ding, B.; Li, B., Biomimetic electrospun nanofibrous structures for tissue engineering. *Mater Today (Kidlington)* **2013**, *16* (6), 229-241.
6. Khang, G.; Lee, S. J.; Kim, M. S.; Lee, H. B., Biomaterials: tissue engineering and scaffolds. *Encyclopedia of Medical devices and instrumentation* **2006**.
7. Ott, H. C.; Matthiesen, T. S.; Goh, S.-K.; Black, L. D.; Kren, S. M.; Netoff, T. I.; Taylor, D. A., Perfusion-decellularized matrix: using nature's platform to engineer a bioartificial heart. *Nature medicine* **2008**, *14* (2), 213.
8. Petersen, T. H.; Calle, E. A.; Zhao, L.; Lee, E. J.; Gui, L.; Raredon, M. B.; Gavrilov, K.; Yi, T.; Zhuang, Z. W.; Breuer, C., Tissue-engineered lungs for in vivo implantation. *Science* **2010**, *329* (5991), 538-541.
9. Cortiella, J.; Niles, J.; Cantu, A.; Brettler, A.; Pham, A.; Vargas, G.; Winston, S.; Wang, J.; Walls, S.; Nichols, J. E., Influence of acellular natural lung matrix on murine embryonic stem cell differentiation and tissue formation. *Tissue Engineering Part A* **2010**, *16* (8), 2565-2580.
10. Kraehenbuehl, T. P.; Zammaretti, P.; Van der Vlies, A. J.; Schoenmakers, R. G.; Lutolf, M. P.; Jaconi, M. E.; Hubbell, J. A., Three-dimensional extracellular matrix-directed cardioprogenitor differentiation: systematic modulation of a synthetic cell-responsive PEG-hydrogel. *Biomaterials* **2008**, *29* (18), 2757-2766.
11. Badylak, S. F. In *The extracellular matrix as a scaffold for tissue reconstruction*, Seminars in cell & developmental biology, Elsevier: 2002; pp 377-383.
12. Rozario, T.; DeSimone, D. W., The extracellular matrix in development and morphogenesis: a dynamic view. *Dev Biol* **2010**, *341* (1), 126-40.
13. Rohman, G., *Biodegradable Polymers: Recent Developments and New Perspectives*. 2017; p 1-454.

14. Frantz, C.; Stewart, K. M.; Weaver, V. M., The extracellular matrix at a glance. *J Cell Sci* **2010**, *123* (24), 4195-4200.
15. Fernandes, H.; Moroni, L.; Van Blitterswijk, C.; De Boer, J., Extracellular matrix and tissue engineering applications. *Journal of materials chemistry* **2009**, *19* (31), 5474-5484.
16. Theocharis, A. D.; Skandalis, S. S.; Gialeli, C.; Karamanos, N. K., Extracellular matrix structure. *Adv Drug Deliv Rev* **2016**, *97*, 4-27.
17. Tsang, K. Y.; Cheung, M. C.; Chan, D.; Cheah, K. S., The developmental roles of the extracellular matrix: beyond structure to regulation. *Cell Tissue Res* **2010**, *339* (1), 93-110.
18. Gordon, M. K.; Hahn, R. A., Collagens. *Cell and tissue research* **2010**, *339* (1), 247.
19. Heino, J., The collagen family members as cell adhesion proteins. *Bioessays* **2007**, *29* (10), 1001-1010.
20. Shoulders, M. D.; Raines, R. T., Collagen structure and stability. *Annu Rev Biochem* **2009**, *78*, 929-58.
21. jeff Hardin, G. P. P., *Becker's World of the Cell*. 9 ed.; Pearson: 2015.
22. Bosman, F. T.; Stamenkovic, I., Functional structure and composition of the extracellular matrix. *The Journal of pathology* **2003**, *200* (4), 423-428.
23. Gelse, K., Collagens—structure, function, and biosynthesis. *Advanced Drug Delivery Reviews* **2003**, *55* (12), 1531-1546.
24. Muiznieks, L. D.; Weiss, A. S.; Keeley, F. W., Structural disorder and dynamics of elastin. *Biochemistry and Cell Biology* **2010**, *88* (2), 239-250.
25. Lucero, H.; Kagan, H., Lysyl oxidase: an oxidative enzyme and effector of cell function. *Cellular and Molecular Life Sciences CMLS* **2006**, *63* (19-20), 2304-2316.
26. McKeown-Longo, P. J., Fibronectin-cell surface interactions. *Reviews of infectious diseases* **1987**, *9* (Supplement_4), S322-S334.
27. Theocharis, A. D.; Skandalis, S. S.; Tzanakakis, G. N.; Karamanos, N. K., Proteoglycans in health and disease: novel roles for proteoglycans in malignancy and their pharmacological targeting. *The FEBS journal* **2010**, *277* (19), 3904-3923.
28. Iozzo, R. V.; Schaefer, L., Proteoglycan form and function: a comprehensive nomenclature of proteoglycans. *Matrix Biology* **2015**, *42*, 11-55.
29. Owen, S. C.; Shoichet, M. S., Design of three-dimensional biomimetic scaffolds. *J Biomed Mater Res A* **2010**, *94* (4), 1321-31.

30. Humphries, J. D.; Byron, A.; Humphries, M. J., Integrin ligands at a glance. *Journal of cell science* **2006**, *119* (19), 3901-3903.
31. Harburger, D. S.; Calderwood, D. A., Integrin signalling at a glance. *Journal of cell science* **2009**, *122* (2), 159-163.
32. Leitinger, B.; Hohenester, E., Mammalian collagen receptors. *Matrix Biology* **2007**, *26* (3), 146-155.
33. Xian, X.; Gopal, S.; Couchman, J. R., Syndecans as receptors and organizers of the extracellular matrix. *Cell and tissue research* **2010**, *339* (1), 31.
34. Dutta, R. C.; Dutta, A. K., Comprehension of ECM-Cell dynamics: A prerequisite for tissue regeneration. *Biotechnology advances* **2010**, *28* (6), 764-769.
35. Zorlutuna, P.; Annabi, N.; Camci-Unal, G.; Nikkhah, M.; Cha, J. M.; Nichol, J. W.; Manbachi, A.; Bae, H.; Chen, S.; Khademhosseini, A., Microfabricated biomaterials for engineering 3D tissues. *Adv Mater* **2012**, *24* (14), 1782-804.
36. Prestwich, G. D., Simplifying the extracellular matrix for 3- D cell culture and tissue engineering: A pragmatic approach. *Journal of cellular biochemistry* **2007**, *101* (6), 1370-1383.
37. Mazzoleni, G.; Di Lorenzo, D.; Steimberg, N., Modelling tissues in 3D: the next future of pharmaco-toxicology and food research? *Genes & nutrition* **2009**, *4* (1), 13.
38. Griffith, L. G.; Swartz, M. A., Capturing complex 3D tissue physiology in vitro. *Nature reviews Molecular cell biology* **2006**, *7* (3), 211.
39. Pampaloni, F.; Reynaud, E. G.; Stelzer, E. H., The third dimension bridges the gap between cell culture and live tissue. *Nature reviews Molecular cell biology* **2007**, *8* (10), 839.
40. Timmins, N.; Harding, F.; Smart, C.; Brown, M.; Nielsen, L., Method for the generation and cultivation of functional three-dimensional mammary constructs without exogenous extracellular matrix. *Cell and tissue research* **2005**, *320* (1), 207-210.
41. Kelm, J. M.; Timmins, N. E.; Brown, C. J.; Fussenegger, M.; Nielsen, L. K., Method for generation of homogeneous multicellular tumor spheroids applicable to a wide variety of cell types. *Biotechnology and bioengineering* **2003**, *83* (2), 173-180.
42. Sachlos, E.; Czernuszka, J., Making tissue engineering scaffolds work. Review: the application of solid freeform fabrication technology to the production of tissue engineering scaffolds. *Eur Cell Mater* **2003**, *5* (29), 39-40.
43. Hutmacher, D. W., Scaffold design and fabrication technologies for engineering tissues—state of the art and future perspectives. *Journal of Biomaterials Science, Polymer Edition* **2001**, *12* (1), 107-124.

44. Ratner, B. D.; Hoffman, A. S.; Schoen, F. J.; Lemons, J. E., *Biomaterials science: an introduction to materials in medicine*. Elsevier: 2004.
45. Lee, C. H.; Singla, A.; Lee, Y., Biomedical applications of collagen. *International journal of pharmaceutics* **2001**, *221* (1-2), 1-22.
46. Parenteau-Bareil, R.; Gauvin, R.; Berthod, F., Collagen-Based Biomaterials for Tissue Engineering Applications. *Materials* **2010**, *3* (3), 1863-1887.
47. Maynes, R., *Structure and function of collagen types*. Elsevier: 2012.
48. Xiang, Z.; Liao, R.; Kelly, M. S.; Spector, M., Collagen–GAG scaffolds grafted onto myocardial infarcts in a rat model: a delivery vehicle for mesenchymal stem cells. *Tissue engineering* **2006**, *12* (9), 2467-2478.
49. Yannas, I.; Lee, E.; Orgill, D. P.; Skrabut, E.; Murphy, G. F., Synthesis and characterization of a model extracellular matrix that induces partial regeneration of adult mammalian skin. *Proceedings of the National Academy of Sciences* **1989**, *86* (3), 933-937.
50. Chamberlain, L.; Yannas, I.; Hsu, H. P.; Strichartz, G.; Spector, M., Near-terminus axonal structure and function following rat sciatic nerve regeneration through a collagen- GAG matrix in a ten- millimeter gap. *Journal of neuroscience research* **2000**, *60* (5), 666-677.
51. Zhang, L.; Yuan, T.; Guo, L.; Zhang, X., An in vitro study of collagen hydrogel to induce the chondrogenic differentiation of mesenchymal stem cells. *Journal of Biomedical Materials Research Part A* **2012**, *100* (10), 2717-2725.
52. Masters, K. S.; Shah, D. N.; Walker, G.; Leinwand, L. A.; Anseth, K. S., Designing scaffolds for valvular interstitial cells: cell adhesion and function on naturally derived materials. *Journal of biomedical materials research Part A* **2004**, *71* (1), 172-180.
53. Alsberg, E.; Feinstein, E.; Joy, M.; Prentiss, M.; Ingber, D. E., Magnetically-guided self-assembly of fibrin matrices with ordered nano-scale structure for tissue engineering. *Tissue engineering* **2006**, *12* (11), 3247-3256.
54. Nair, L. S.; Laurencin, C. T., Biodegradable polymers as biomaterials. *Progress in Polymer Science* **2007**, *32* (8-9), 762-798.
55. Hubbell, J. A., Biomaterials in tissue engineering. *Nature Biotechnology* **1995**, *13* (6), 565.
56. Rosso, F.; Giordano, A.; Barbarisi, M.; Barbarisi, A., From cell–ECM interactions to tissue engineering. *Journal of cellular physiology* **2004**, *199* (2), 174-180.
57. Kim, B.-S.; Mooney, D. J., Engineering smooth muscle tissue with a predefined structure. **1998**.

58. Khang, G.; Lee, S. J.; Han, C. W.; Rhee, J. M.; Lee, H. B., Preparation and characterization of natural/synthetic hybrid scaffolds. In *Tissue Engineering, Stem Cells, and Gene Therapies*, Springer: 2003; pp 235-245.
59. Peters, M.; Mooney, D. In *Synthetic Extracellular Matrices for Cell Transplantation*, Materials science forum, Trans Tech Publ: 1997; pp 43-52.
60. Yang, S.; Leong, K.-F.; Du, Z.; Chua, C.-K., The design of scaffolds for use in tissue engineering. Part I. Traditional factors. *Tissue engineering* **2001**, *7* (6), 679-689.
61. Yang, F.; Murugan, R.; Ramakrishna, S.; Wang, X.; Ma, Y.-X.; Wang, S., Fabrication of nano-structured porous PLLA scaffold intended for nerve tissue engineering. *Biomaterials* **2004**, *25* (10), 1891-1900.
62. Gunatillake, P. A.; Adhikari, R., Biodegradable synthetic polymers for tissue engineering. *Eur Cell Mater* **2003**, *5* (1), 1-16.
63. Lemmouchi, Y.; Schacht, E., Preparation and in vitro evaluation of biodegradable poly (ϵ -caprolactone-co-d, l lactide)(XY) devices containing trypanocidal drugs. *Journal of controlled release* **1997**, *45* (3), 227-233.
64. Huang, M. H.; Li, S.; Coudane, J.; Vert, M., Synthesis and Characterization of Block Copolymers of ϵ - Caprolactone and DL- Lactide Initiated by Ethylene Glycol or Poly (ethylene glycol). *Macromolecular chemistry and physics* **2003**, *204* (16), 1994-2001.
65. Li, Y.; Zhu, K.; Zhang, J.; Jiang, H.; Liu, J.; Hao, Y.; Yasuda, H.; Ichimaru, A.; Yamamoto, K., In vitro and in vivo studies of cyclosporin A-loaded microspheres based on copolymers of lactide and ϵ -caprolactone: Comparison with conventional PLGA microspheres. *International journal of pharmaceutics* **2005**, *295* (1-2), 67-76.
66. Ruckh, T. T.; Kumar, K.; Kipper, M. J.; Papat, K. C., Osteogenic differentiation of bone marrow stromal cells on poly (ϵ -caprolactone) nanofiber scaffolds. *Acta biomaterialia* **2010**, *6* (8), 2949-2959.
67. Chen, L.; Bai, Y.; Liao, G.; Peng, E.; Wu, B.; Wang, Y.; Zeng, X.; Xie, X., Electrospun poly (L-lactide)/poly (ϵ -caprolactone) blend nanofibrous scaffold: characterization and biocompatibility with human adipose-derived stem cells. *PLoS One* **2013**, *8* (8), e71265.
68. Xie, J.; Ihara, M.; Jung, Y.; Kwon, I. K.; Kim, S. H.; Kim, Y. H.; Matsuda, T., Mechano-active scaffold design based on microporous poly (L-lactide-co- ϵ -caprolactone) for articular cartilage tissue engineering: Dependence of porosity on compression force-applied mechanical behaviors. *Tissue engineering* **2006**, *12* (3), 449-458.
69. Xie, J.; Jung, Y.; Kim, S. H.; Kim, Y. H.; Matsuda, T., New Technique of Seeding Chondrocytes into Microporous Poly (L-lactide-co- ϵ -caprolactone) Sponge by Cyclic Compression Force-Induced Suction. *Tissue engineering* **2006**, *12* (7), 1811-1820.

70. Bhang, S. H.; Jeong, S. I.; Lee, T. J.; Jun, I.; Lee, Y. B.; Kim, B. S.; Shin, H., Electroactive Electrospun Polyaniline/Poly [(L- lactide)- co- (ϵ - caprolactone)] Fibers for Control of Neural Cell Function. *Macromolecular bioscience* **2012**, *12* (3), 402-411.
71. Jeong, S. I.; Kim, S. H.; Kim, Y. H.; Jung, Y.; Kwon, J. H.; Kim, B.-S.; Lee, Y. M., Manufacture of elastic biodegradable PLCL scaffolds for mechano-active vascular tissue engineering. *Journal of Biomaterials Science, Polymer Edition* **2004**, *15* (5), 645-660.
72. Mo, X. M.; Xu, C. Y.; Kotaki, M.; Ramakrishna, S., Electrospun P(LLA-CL) nanofiber: a biomimetic extracellular matrix for smooth muscle cell and endothelial cell proliferation. *Biomaterials* **2004**, *25* (10), 1883-1890.
73. Vaquette, C.; Frochet, C.; Rahouadj, R.; Muller, S.; Wang, X., Mechanical and biological characterization of a porous poly- L- lactic acid- co- ϵ - caprolactone scaffold for tissue engineering. *Soft Materials* **2008**, *6* (1), 25-33.
74. Laurent, C. P.; Vaquette, C.; Liu, X.; Schmitt, J. F.; Rahouadj, R., Suitability of a PLCL fibrous scaffold for soft tissue engineering applications: A combined biological and mechanical characterisation. *J Biomater Appl* **2018**, *32* (9), 1276-1288.
75. Göpferich, A., Polymer bulk erosion. *Macromolecules* **1997**, *30* (9), 2598-2604.
76. Zhang, Y.; Venugopal, J.; Huang, Z.-M.; Lim, C.; Ramakrishna, S., Characterization of the surface biocompatibility of the electrospun PCL-collagen nanofibers using fibroblasts. *Biomacromolecules* **2005**, *6* (5), 2583-2589.
77. Rentsch, C.; Rentsch, B.; Heinemann, S.; Bernhardt, R.; Bischoff, B.; Forster, Y.; Scharnweber, D.; Rammelt, S., ECM inspired coating of embroidered 3D scaffolds enhances calvaria bone regeneration. *Biomed Res Int* **2014**, *2014*, 217078.
78. Joo, S.; Kim, J. Y.; Lee, E.; Hong, N.; Sun, W.; Nam, Y., Effects of ECM protein micropatterns on the migration and differentiation of adult neural stem cells. *Sci Rep* **2015**, *5*, 13043.
79. Subia, B.; Kundu, J.; Kundu, S., Biomaterial scaffold fabrication techniques for potential tissue engineering applications. In *Tissue engineering*, InTech: 2010.
80. Mikos, A. G.; Bao, Y.; Cima, L. G.; Ingber, D. E.; Vacanti, J. P.; Langer, R., Preparation of poly (glycolic acid) bonded fiber structures for cell attachment and transplantation. *Journal of Biomedical Materials Research Part A* **1993**, *27* (2), 183-189.
81. Mikos, A. G.; Sarakinos, G.; Leite, S. M.; Vacanti, J. P.; Langer, R., Laminated three-dimensional biodegradable foams for use in tissue engineering. *The Biomaterials: Silver Jubilee Compendium* **1993**, *14*, 93-100.
82. Mikos, A. G.; Sarakinos, G.; Vacanti, J. P.; Langer, R. S.; Cima, L. G., Biocompatible polymer membranes and methods of preparation of three dimensional membrane structures. Google Patents: 1996.

83. Mikos, A. G.; Thorsen, A. J.; Czerwonka, L. A.; Bao, Y.; Langer, R.; Winslow, D. N.; Vacanti, J. P., Preparation and characterization of poly (L-lactic acid) foams. *Polymer* **1994**, *35* (5), 1068-1077.
84. Mehrabian, M.; Nasr-Esfahani, M., HA/nylon 6, 6 porous scaffolds fabricated by salt-leaching/solvent casting technique: effect of nano-sized filler content on scaffold properties. *International journal of nanomedicine* **2011**, *6*, 1651.
85. DI, S. E. C. DEVELOPMENT AND CHARACTERISATION OF 3D-SCAFFOLDS MIMICKING THE BONE MARROW NICHE FOR BLAST CELL CULTURE. UNIVERSITY OF MODENA AND REGGIO EMILIA, 2016.
86. Quirk, R. A.; France, R. M.; Shakesheff, K. M.; Howdle, S. M., Supercritical fluid technologies and tissue engineering scaffolds. *Current Opinion in Solid State and Materials Science* **2004**, *8* (3-4), 313-321.
87. Zellander, A.; Gemeinhart, R.; Djalilian, A.; Makhsous, M.; Sun, S.; Cho, M., Designing a gas foamed scaffold for keratoprosthesis. *Materials Science and Engineering: C* **2013**, *33* (6), 3396-3403.
88. Haugen, H.; Ried, V.; Brunner, M.; Will, J.; Wintermantel, E., Water as foaming agent for open cell polyurethane structures. *Journal of Materials Science: Materials in Medicine* **2004**, *15* (4), 343-346.
89. Bajaj, P.; Schweller, R. M.; Khademhosseini, A.; West, J. L.; Bashir, R., 3D biofabrication strategies for tissue engineering and regenerative medicine. *Annu Rev Biomed Eng* **2014**, *16*, 247-76.
90. Zhu, N.; Chen, X., Biofabrication of tissue scaffolds. In *Advances in biomaterials science and biomedical applications*, InTech: 2013.
91. Wittmer, C. R.; Hu, X.; Gauthier, P. C.; Weisman, S.; Kaplan, D. L.; Sutherland, T. D., Production, structure and in vitro degradation of electrospun honeybee silk nanofibers. *Acta Biomater* **2011**, *7* (10), 3789-95.
92. Huang, Z.-M.; Zhang, Y.-Z.; Kotaki, M.; Ramakrishna, S., A review on polymer nanofibers by electrospinning and their applications in nanocomposites. *Composites science and technology* **2003**, *63* (15), 2223-2253.
93. Lam, C. X. F.; Mo, X.; Teoh, S.-H.; Hutmacher, D., Scaffold development using 3D printing with a starch-based polymer. *Materials Science and Engineering: C* **2002**, *20* (1-2), 49-56.
94. Arslan-Yildiz, A.; El Assal, R.; Chen, P.; Guven, S.; Inci, F.; Demirci, U., Towards artificial tissue models: past, present, and future of 3D bioprinting. *Biofabrication* **2016**, *8* (1), 014103.
95. Karalekas, D., Study of the mechanical properties of nonwoven fibre mat reinforced photopolymers used in rapid prototyping. *Materials & design* **2003**, *24* (8), 665-670.

96. Wiria, F.; Leong, K.; Chua, C.; Liu, Y., Poly- ϵ -caprolactone/hydroxyapatite for tissue engineering scaffold fabrication via selective laser sintering. *Acta biomaterialia* **2007**, *3* (1), 1-12.
97. Hutmacher, D. W.; Schantz, T.; Zein, I.; Ng, K. W.; Teoh, S. H.; Tan, K. C., Mechanical properties and cell cultural response of polycaprolactone scaffolds designed and fabricated via fused deposition modeling. *Journal of Biomedical Materials Research Part A* **2001**, *55* (2), 203-216.
98. Hutmacher, D. W., Scaffolds in tissue engineering bone and cartilage. *Biomaterials* **2000**, *21* (24), 2529-43.
99. Kai, H.; Wang, X.; Madhukar, K. S.; Qin, L.; Yan, Y.; Zhang, R.; Wang, X., Fabrication of a two-level tumor bone repair biomaterial based on a rapid prototyping technique. *Biofabrication* **2009**, *1* (2), 025003.
100. Formhals, A., Process and apparatus for preparing artificial threads.. US Patent, 1975504. 1934.
101. Formhals, A., Method and apparatus for spinning (US, 2160962). 1939.
102. Anton, F., Artificial thread and method of producing same. Google Patents: 1940.
103. Anton, F., Production of artificial fibers from fiber forming liquids. Google Patents: 1943.
104. Anton, F., Method and apparatus for spinning. Google Patents: 1944.
105. Bhardwaj, N.; Kundu, S. C., Electrospinning: a fascinating fiber fabrication technique. *Biotechnology advances* **2010**, *28* (3), 325-347.
106. Valizadeh, A.; Farkhani, S. M., Electrospinning and electrospun nanofibres. *IET nanobiotechnology* **2013**, *8* (2), 83-92.
107. Gibson, P.; Schreuder-Gibson, H.; Rivin, D., Transport properties of porous membranes based on electrospun nanofibers. *Colloids and Surfaces A: Physicochemical and Engineering Aspects* **2001**, *187*, 469-481.
108. Tsai, P. P.; Schreuder-Gibson, H.; Gibson, P., Different electrostatic methods for making electret filters. *Journal of Electrostatics* **2002**, *54* (3-4), 333-341.
109. Buchko, C. J.; Chen, L. C.; Shen, Y.; Martin, D. C., Processing and microstructural characterization of porous biocompatible protein polymer thin films. *Polymer* **1999**, *40* (26), 7397-7407.
110. He, X.; Cheng, L.; Zhang, X.; Xiao, Q.; Zhang, W.; Lu, C., Tissue engineering scaffolds electrospun from cotton cellulose. *Carbohydr Polym* **2015**, *115*, 485-93.

111. Zong, X.; Kim, K.; Fang, D.; Ran, S.; Hsiao, B. S.; Chu, B., Structure and process relationship of electrospun bioabsorbable nanofiber membranes. *Polymer* **2002**, *43* (16), 4403-4412.
112. Dong, R. H.; Jia, Y. X.; Qin, C. C.; Zhan, L.; Yan, X.; Cui, L.; Zhou, Y.; Jiang, X.; Long, Y. Z., In situ deposition of a personalized nanofibrous dressing via a handy electrospinning device for skin wound care. *Nanoscale* **2016**, *8* (6), 3482-8.
113. Sridhar, R.; Lakshminarayanan, R.; Madhaiyan, K.; Barathi, V. A.; Lim, K. H. C.; Ramakrishna, S., Electrospayed nanoparticles and electrospun nanofibers based on natural materials: applications in tissue regeneration, drug delivery and pharmaceuticals. *Chemical Society Reviews* **2015**, *44* (3), 790-814.
114. Kontogiannopoulos, K. N.; Assimopoulou, A. N.; Tsivintzelis, I.; Panayiotou, C.; Papageorgiou, V. P., Electrospun fiber mats containing shikonin and derivatives with potential biomedical applications. *International journal of pharmaceutics* **2011**, *409* (1-2), 216-228.
115. Jiang, T.; Carbone, E. J.; Lo, K. W. H.; Laurencin, C. T., Electrospinning of polymer nanofibers for tissue regeneration. *Progress in Polymer Science* **2015**, *46*, 1-24.
116. Raghavan, P.; Lim, D.-H.; Ahn, J.-H.; Nah, C.; Sherrington, D. C.; Ryu, H.-S.; Ahn, H.-J., Electrospun polymer nanofibers: the booming cutting edge technology. *Reactive and Functional Polymers* **2012**, *72* (12), 915-930.
117. Thavasi, V.; Singh, G.; Ramakrishna, S., Electrospun nanofibers in energy and environmental applications. *Energy & Environmental Science* **2008**, *1* (2), 205-221.
118. Subbiah, T.; Bhat, G.; Tock, R.; Parameswaran, S.; Ramkumar, S., Electrospinning of nanofibers. *Journal of Applied Polymer Science* **2005**, *96* (2), 557-569.
119. Kwon, I. K.; Matsuda, T., Co-electrospun nanofiber fabrics of poly (L-lactide-co- ϵ -caprolactone) with type I collagen or heparin. *Biomacromolecules* **2005**, *6* (4), 2096-2105.
120. Fang, Z.; Fu, W.; Dong, Z.; Zhang, X.; Gao, B.; Guo, D.; He, H.; Wang, Y., Preparation and biocompatibility of electrospun poly(l-lactide-co- ϵ -caprolactone)/fibrinogen blended nanofibrous scaffolds. *Applied Surface Science* **2010**, *257* (9), 4133-4138.
121. Yin, A.; Zhang, K.; McClure, M. J.; Huang, C.; Wu, J.; Fang, J.; Mo, X.; Bowlin, G. L.; Al-Deyab, S. S.; El-Newehy, M., Electrospinning collagen/chitosan/poly (L-lactic acid-co- ϵ -caprolactone) to form a vascular graft: Mechanical and biological characterization. *Journal of biomedical materials research Part A* **2013**, *101* (5), 1292-1301.
122. He, X.; Fu, W.; Feng, B.; Wang, H.; Liu, Z.; Yin, M.; Wang, W.; Zheng, J., Electrospun collagen-poly (L-lactic acid-co- ϵ -caprolactone) membranes for cartilage tissue engineering. *Regenerative medicine* **2013**, *8* (4), 425-436.

123. Du, L.; Xu, H.; Zhang, Y.; Zou, F., Electrospinning of polycaprolatone nanofibers with DMF additive: The effect of solution proprieties on jet perturbation and fiber morphologies. *Fibers and Polymers* **2016**, *17* (5), 751-759.
124. Casasola, R.; Thomas, N. L.; Trybala, A.; Georgiadou, S., Electrospun poly lactic acid (PLA) fibres: Effect of different solvent systems on fibre morphology and diameter. *Polymer* **2014**, *55* (18), 4728-4737.
125. Chung, S.; Moghe, A. K.; Montero, G. A.; Kim, S. H.; King, M. W., Nanofibrous scaffolds electrospun from elastomeric biodegradable poly(L-lactide-co-epsilon-caprolactone) copolymer. *Biomed Mater* **2009**, *4* (1), 015019.
126. Haider, A.; Haider, S.; Kang, I.-K., A comprehensive review summarizing the effect of electrospinning parameters and potential applications of nanofibers in biomedical and biotechnology. *Arabian Journal of Chemistry* **2015**.
127. Matthews, J. A.; Wnek, G. E.; Simpson, D. G.; Bowlin, G. L., Electrospinning of collagen nanofibers. *Biomacromolecules* **2002**, *3* (2), 232-238.
128. Ekaputra, A. K.; Prestwich, G. D.; Cool, S. M.; Hutmacher, D. W., The three-dimensional vascularization of growth factor-releasing hybrid scaffold of poly (epsilon-caprolactone)/collagen fibers and hyaluronic acid hydrogel. *Biomaterials* **2011**, *32* (32), 8108-17.
129. Xu, Y.; Wu, J.; Wang, H.; Li, H.; Di, N.; Song, L.; Li, S.; Li, D.; Xiang, Y.; Liu, W.; Mo, X.; Zhou, Q., Fabrication of electrospun poly(L-lactide-co-epsilon-caprolactone)/collagen nanoyarn network as a novel, three-dimensional, macroporous, aligned scaffold for tendon tissue engineering. *Tissue Eng Part C Methods* **2013**, *19* (12), 925-36.
130. He, X.; Fu, W.; Feng, B.; Wang, H.; Liu, Z.; Yin, M.; Wang, W.; Zheng, J., Electrospun Collagen/Poly(L-lactic acid-co-epsilon-caprolactone) Hybrid Nanofibrous Membranes Combining with Sandwich Construction Model for Cartilage Tissue Engineering. *Journal of Nanoscience and Nanotechnology* **2013**, *13* (6), 3818-3825.
131. Zhang, K.; Wang, H.; Huang, C.; Su, Y.; Mo, X.; Ikada, Y., Fabrication of silk fibroin blended P(LLA-CL) nanofibrous scaffolds for tissue engineering. *J Biomed Mater Res A* **2010**, *93* (3), 984-93.
132. Menzies, K. L.; Jones, L., The impact of contact angle on the biocompatibility of biomaterials. *Optometry and Vision Science* **2010**, *87* (6), 387-399.
133. Stutzenberger, F. J., Interference of the Detergent Tween 80 in Protein Assays. *Analytical Biochemistry* **1992**, *207* (2), 249-254.
134. Agarkhed, M.; O'Dell, C.; Hsieh, M. C.; Zhang, J.; Goldstein, J.; Srivastava, A., Effect of polysorbate 80 concentration on thermal and photostability of a monoclonal antibody. *AAPS PharmSciTech* **2013**, *14* (1), 1-9.

135. Saha, S. K.; Tsuji, H., Effects of rapid crystallization on hydrolytic degradation and mechanical properties of poly (l-lactide-co- ϵ -caprolactone). *Reactive and Functional Polymers* **2006**, *66* (11), 1362-1372.
136. Matta, A.; Rao, R. U.; Suman, K.; Rambabu, V., Preparation and characterization of biodegradable PLA/PCL polymeric blends. *Procedia Materials Science* **2014**, *6*, 1266-1270.
137. Heimowska, A.; Morawska, M.; Bocho-Janiszewska, A., Biodegradation of poly (ϵ -caprolactone) in natural water environments. *Polish Journal of Chemical Technology* **2017**, *19* (1), 120-126.
138. Ahola, N.; Veiranto, M.; Rich, J.; Efimov, A.; Hannula, M.; Seppala, J.; Kellomaki, M., Hydrolytic degradation of composites of poly(L-lactide-co-epsilon-caprolactone) 70/30 and beta-tricalcium phosphate. *J Biomater Appl* **2013**, *28* (4), 529-43.